Behavior of the Laplacian of Gaussian Extrema

Salvatore Tabbone, Laurent Alonso, Djemel Ziou

Behavior of the Laplacian of Gaussian Extrema

S.A. Tabbone[1], L. Alonso and D. Ziou
Loria-UMR n^o 7503-University of Nancy2-INRIA Lorraine,
Campus Scientifique,
BP 239, 54506 Vandœuvre-Les-Nancy, France, Fax (33) 3 83 41 30 79
email{tabbone,alonso@loria.fr}

June 20, 2003

[1]Corresponding author.

0.1 keywords

Laplacian Extrema, Gaussian Filtering, Scale Space.

0.2 Abstract

This paper analyses the behavior in scale space of linear junction models (L, Y and X models), nonlinear junction models, and linear junction multi-models. The variation of grey level is considered to be constant, linear or nonlinear in the case of linear models and constant for the other models. We are essentially interested in the extrema points provided by the Laplacian of Gaussian function. These extrema have nice scaling properties and can be used for detecting junction points, for tracking or indexing images. Moreover, we show that for infinite models the Laplacian of the Gaussian at the corner point is not always equal to zero.

0.3 Introduction

Early vision begins with the computation of a compact description of the raw image intensity. The ultimate purpose of the initial description is to capture all the significant properties of objects present in the image. Physical edges provide important visual information since they correspond to the discontinuities of the physical, photometrical and geometrical properties of the objects. They are represented in the image by changes (1D or 2D) in the intensity function. Junctions are extremely useful 2D features. They are of great use for solving correspondence problems in computer vision. Various methods have been proposed for detecting corners [21, 24, 25]. In some cases, the image is segmented into digital curves and a corner corresponds to a maximum of curvature [2, 8, 13, 15]. Other approaches operate directly on grey level images and take into account differential properties of the image intensities to measure the curvature of an edge [4, 9, 12, 14, 20, 26, 28]. In some cases the local intensity function of the corner is characterized [1, 6, 10, 11, 16]. Several approaches are based on the strength of the modulus of the gradient vector to select corner candidates or to compute the curvature. However, at the junction point the value of the modulus is weak [5]. The zero-crossings of the Laplacian of Gaussian have been used to locate junction points [7] too. It has been shown that the Laplacian of Gaussian at the linear corner model with a constant illumination and infinite extent equals zero [3, 5].

Several studies have been dedicated on the precision in estimating the location of edges or corners caused by local operators or noisy data [17, 18]. Furthermore geometrical properties of the detection of corners or trihedral vertices with zero-crossings have been analyzed in [3, 5]. However the properties to nonlinear junction models has not been studied.

In this paper we are particularly interested by the Laplacian of Gaussian extrema. We focus our attention to these points because they have nice scaling properties and can be used for detecting junction points. The extrema of the Laplacian have been first used in [23] to detect junction points or to decrease the time and the memory

requirements of 3D differential corner detectors [22]. In these works, the extremum has been numerically underlined only for a corner with a constant illumination and infinite extent.

We consider three junction models that are more frequently encountered in real images: general linear junction, nonlinear junction, and linear junction multi-models. The variation of grey level is considered to be constant, linear or nonlinear. We prove that a corner with constant illumination and infinite extent provides an extremum inside the corner sector. This property is checked numerically for all the other junction models. Furthermore, we show that for infinite models the value of the Laplacian at the corner point is not always equal to zero . More precisely, the response at the corner point relies on the degree of linearity of the model and the illumination.

First we give some notations (section 2) and we study the behavior of L-junction models (section 3). We prove some properties on the junctions and extremal points. The demonstration are given in Appendix A and B. Then, some of these properties are checked on more complex models (section 4 and 5). Perspectives of our work are given in conclusion.

0.4 Notations

Let g denote the one-dimensional Gaussian filter,

$$g(x) = \frac{1}{\sqrt{2\pi}\sigma} e^{-\frac{x^2}{2\sigma^2}},$$

with ϕ being the error function,

$$\phi(x) = \int_{-\infty}^{x} g(t)dt,$$

G the two-dimensional Gaussian,

$$G(x, y) = g(x)g(y),$$

and H the Heaviside function,

$$H(x) = \begin{cases} 0 & \text{if } x \leq 0 \\ 1 & \text{if } x > 0 \end{cases} .$$

To simplify the notation, we state F_x, F_y, F_{xx} and F_{yy} be the partial derivatives of F that is, $\frac{\partial F}{\partial x}$, $\frac{\partial F}{\partial y}$, $\frac{\partial^2 F}{\partial x^2}$ and $\frac{\partial^2 F}{\partial y^2}$.

0.5 L-junctions behavior

In this section, we study the behavior of the Laplacian of Gaussian for four L-junction models also called corners (see Table 1) and which are mostly encountered in an image. The models are linear and nonlinear and the illumination is considered to be constant

and non-constant. The first model (see Table 1.a) is the classical corner model which is commonly used on the ground of several corner detectors. For this model we prove that the Laplacian of Gaussian gives rise to an extremum inside the corner sector.

In reality however, the illumination is not constant. Mutual illumination and specularities are quite usual and their effects are particularly significant in the vicinity of convex or concave object contours. These models (see Table 1.d and g) commonly appear in range images or in medical imagery. Moreover in the real world objects are not necessarily polyhedral but curved (see Table 1.j). Due to the complexity of these models we check numerically the presence of the extremum. However we prove that for some infinite models the Laplacian is not zero at the corner point. Furthermore for clarity of presentation these models have been selected with a right angle. The extension to any angle is easily to do by applying a rotation transform on the x and y variables.

0.5.1 Definition of L-models

Following the theorem of convolution, on each model I we calculate:

$$F(x,y) = (G * I)(x,y) = \int_{-\infty}^{\infty}\int_{-\infty}^{\infty} I(x-\epsilon, y-\eta)G(\epsilon,\eta)d\epsilon d\eta,$$

and we define the Laplacian of F by : $\nabla^2 F(x,y) = F_{xx} + F_{yy}$. Let the four intensity models be:

- **Models with straight edges and constant intensity variation**

  $$I(x,y) = (A_1 - A_0) \times H(y\cos(\theta_0) - x\sin(\theta_0)) \times H(x\sin(\theta_1) - y\cos(\theta_1)) + A_0,$$

  where $-\frac{\pi}{2} < \theta_0 < \theta_1 < \frac{\pi}{2}$. $(\theta_1 - \theta_0)$ and $(A_1 - A_0)$ are respectively the aperture and the amplitude of the L-junction (see Table 1.a). We have (details are given in Appendix A) :

  $$F(x,y) = (A_1 - A_0)\int_{\epsilon=-\infty}^{x} g(\epsilon)(\phi(y-(x-\epsilon)\tan\theta_0) - \phi(y-(x-\epsilon)\tan\theta_1))d\epsilon + A_0,$$

  and :

  $$\nabla^2 F(x,y) = \frac{1}{\sigma^2}\sum_{i=0}^{1}(A_i - A_{((i+1) \bmod 2)})u_i g(u_i)\phi(v_i), \qquad (1)$$

  where $u_i = y\cos(\theta_i) - x\sin(\theta_i)$ and $v_i = x\cos(\theta_i) + y\sin(\theta_i)$. At the corner point, we have : $\nabla^2 F(0,0) = 0$.

- **Models with straight edges and linear intensity variation**

  $$I(x,y) = H(x)H(y)(1 + Kx + Ky),$$

  where K is a measure of the slope linearity of the illumination (see Table 1.d).

  $$F(x,y) = \phi(x)\phi(y)(1 + Kx + Ky) + K\sigma^2(g(x)\phi(y) + g(y)\phi(x)),$$

$$\nabla^2 F(x,y) = -Kg(x)g(y)(x+y)+g(x)\phi(y)(K-\frac{x}{\sigma^2}(1+Ky))+g(y)\phi(x)(K-\frac{y}{\sigma^2}(1+Kx))$$

At the corner point, we have : $\nabla^2 F(0,0) = \frac{K}{\sqrt{2\pi}\sigma}$

- **Models with straight edges and nonlinear intensity variation**

$$I(x,y) = H(x)H(y)(1+Kx^2+Ky^2),$$

where K is a measure of the nonlinearity of the illumination (see Table 1.g).

$$F(x,y) = \phi(x)\phi(y)(1+K(2\sigma^2+x^2+y^2))+K\sigma^2(xg(x)\phi(y)+yg(y)\phi(x)),$$

$$\nabla^2 F(x,y) = -2Kxyg(x)g(y)+4K\phi(x)\phi(y)-$$

$$\frac{1}{\sigma^2}\left(xg(x)\phi(y)(1+Ky^2+K\sigma^2)+yg(y)\phi(x)(1+Kx^2+K\sigma^2)\right)$$

At the corner point : $\nabla^2 F(0,0) = K$

- **Models with curved straight edges and constant intensity variation**

$$I(x,y) = H(x)H(-y+Kx^2)H(y+Kx^2),$$

where K is the slope of the tangent line at the origin (see Table 1.i).

$$F(x,y) = \int_0^\infty g(x-\alpha)\phi(y-K\alpha^2)d\alpha - \int_0^\infty g(x-\alpha)\phi(y+K\alpha^2)d\alpha,$$

$$\nabla^2 F(x,y) = \frac{1}{\sigma^2}\int_0^\infty g(x-\alpha)(((x-\alpha)^2-\sigma^2)(\phi(y-K\alpha^2)-\phi(y+K\alpha^2))+$$

$$((y+K\alpha^2)g(y+K\alpha^2)-(y-K\alpha^2)g(y-K\alpha^2)))d\alpha$$

We have :

$$\nabla^2 F(0,0) = -\frac{K}{\pi\sigma^4}\int_0^\infty \alpha^2 e^{-\frac{\alpha^2}{2\sigma^2}} e^{-\frac{K^2\alpha^4}{2\sigma^2}} d\alpha \qquad (2)$$

Since all the models are symmetric according to their bisector line, for each model we have the following proposition:

Proposition 1 *For all the points on the corner bisector, the gradient orientation is the same as the corner bisector.*

For the model with constant intensity, we have :

Proposition 2 *$\nabla^2 F(x,y)$ provides inside the corner sector on the bisector line a point $P_1 = (x_1, \tan\left(\frac{\theta_1+\theta_0}{2}\right)x_1)$ with $\frac{\sigma}{\sin(\frac{(\theta_1-\theta_0)}{2})} < x_1 < \frac{\sqrt{3}\sigma}{\sin(\frac{(\theta_1-\theta_0)}{2})}$ which corresponds to the only extremum of $\nabla^2 F(x,y)$ (see Table 1.a-c). We also have $\nabla^2 F_{P_1} = \Theta\left(\frac{A_1-A_0}{\sigma^2}\right)$.*

The proof of this proposition is given in Appendix B (cf Corollary 1 and 3). By the way we demonstrate in the Appendix B that there is an other characteristic point on the bisector line which is a hyperbolic point. Here we focus our attention only on the extremum point because this point has nice scaling properties and can be easily detected in the discrete case (a local maximum for a dark corner on a light background or a local minimum for a light corner on a dark background).

From the previous proposition, we can say that :

- The response of the Laplacian of Gaussian at the extremum is a function of the scale and the contrast between the sectors.
- The position of this point depends on the scale σ and the corner aperture $(\theta_1 - \theta_0)$, that is, this point moves away from the corner when the scale increases or the corner aperture decreases.

Table 2.a illustrates the position of the extremum according to the scale.

For the other models we have checked numerically the presence of an extremum inside the corner sector on the bisector line (see Table 1). The position of the extremum as a function of the scale has been numerically verified for these models too (see Table 2). From numerical calculations, it seems that this point is the only extremum of $\nabla^2 F$.

Moreover, we can remark that the Laplacian is zero at the corner point only for the model with constant intensity. We can see that when K approaches zero in these two models with non-constant illumination, the intensities models become constant. In this case the corresponding Laplacian responses at the corner points equal to zero. Moreover for the model with non-linear intensity, we can remark from Table 3.c the creation of one spurious edge due to the degree of nonlinearity of the model. This kind of spurious contours have been also underlined in [3] for the case of infinite straight edge model with nonlinear illumination.

When the model has curved edges, the value at the corner point relies on the degree of curvature at that point. More precisely, when $K \to \infty$ the model is less curved and it describes a step edge (the tangent line at the origin is infinite). In this case the formula (2) can be rewritten (where $u = \frac{\alpha\sqrt{K}}{\sigma}$) :

$$\lim_{K\to\infty} \nabla^2 F(0,0) = \lim_{K\to\infty} \frac{1}{\sqrt{K}\sigma} \int_0^\infty -u^2 e^{\frac{-u^4\sigma^2}{2}} e^{\frac{-u^2}{2K}} du \to 0$$

0.6 Multi L-junctions

In this section we provide two models (an infinite model and a closed one) having several adjacent L-models. These models have been selected because in an image the corner is rarely alone. The creation of an extremum in the vicinity of the corner is also verified for these models.

3D model	Laplacian of Gaussian response	1D profile on the line bisector
a. 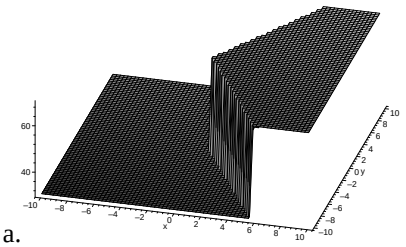	b. 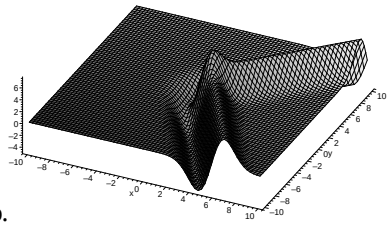	c. 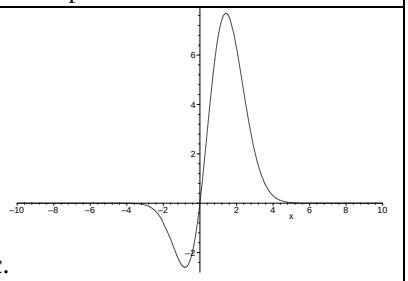
d. 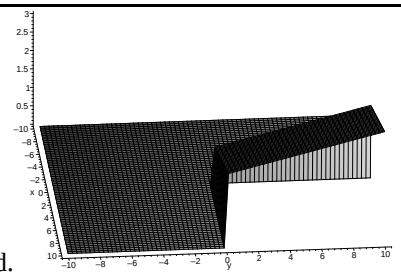	e. 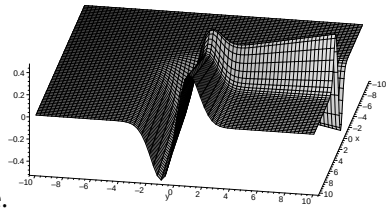	f. 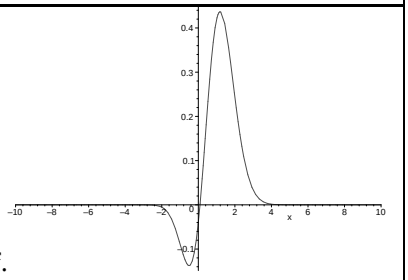
g. 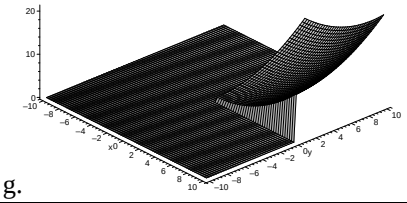	h. 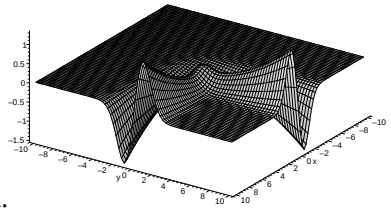	i. 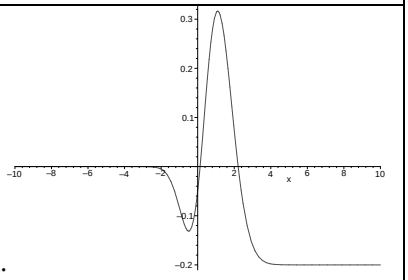
j. 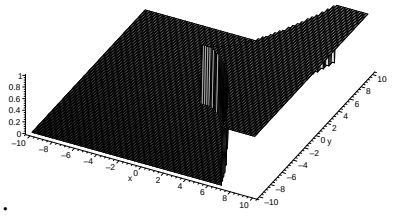	k. 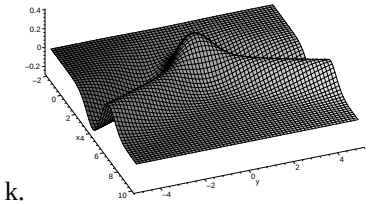	l. 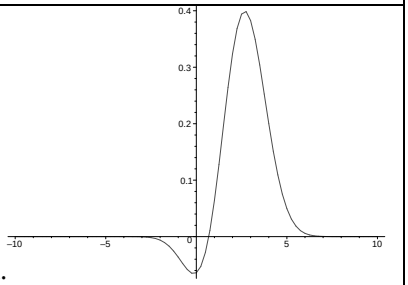

Table 1: Behavior of the extrema for L-corners.
For all the responses $\sigma = 1$. *a)* $A_1 - A_0 = 10, \theta_1 = \frac{\pi}{3}$ *and* $\theta_0 = -\frac{\pi}{3}$. *d)* $K = 0.1$. *h)*$K = 0.05$. *k)* $K = 0.2$.

0.6.1 Definitions

Let $u = y\cos(\theta) - x\sin(\theta)$, $v = y\sin(\theta) + x\cos(\theta)$ and let the two following models be :

- **Infinite model**

$$I(x,y) = H(x)H(W-x)H(\tan(\theta)x - y),$$

where W and θ are respectively the width and the slope of the model (see figure 1).

$$F(x,y) = \phi(x) - \phi(x-W) - \int_{x-W}^{x} g(\alpha)\phi(y - \tan(\theta)(x-\alpha))d\alpha,$$

$$\nabla^2 F(x,y) = \frac{1}{\sigma^2}(xg(x)(\phi(y)-1) + (x-W)g(x-W)(1-\phi(y-W\tan(\theta))) +$$

$$ug(u)(\phi(v) - \phi(v - \frac{W}{\cos(\theta)})))$$

At the corner points $P_1 = (0,0)$ and $P_2 = (W, W\tan(\theta))$ the Laplacian is :

$$\nabla^2 F(0,0) = -\frac{Wg(W)\phi(W\tan(\theta))}{\sigma^2}$$

and

$$\nabla^2 F(W, W\tan(\theta)) = -\frac{Wg(W)\phi(-W\tan(\theta))}{\sigma^2}.$$

- **Finite model**

$$I(x,y) = H(x)H(y)H(W-x)H(\tan(\theta)x - y),$$

$$F(x,y) = \phi(y)(\phi(x) - \phi(x-W)) - \int_{x-W}^{x} g(\alpha)\phi(y - \tan(\theta)(x-\alpha))d\alpha,$$

where W and θ are respectively the width and the slope of the model (see figure 4).

$$\nabla^2 F(x,y) = \frac{1}{\sigma^2}(-yg(y)(\phi(x)-\phi(x-W)) + (x-W)g(x-W)(\phi(y)-\phi(y-W\tan(\theta))) +$$

$$ug(u)(\phi(v) - \phi(v - \frac{W}{\cos(\theta)}))).$$

This model has three corners $P_0 = (0,0), P_1 = (W,0)$ and $P_2 = (W, \tan(\theta)W)$ and the Laplacian is:

$$\nabla^2 F(0,0) = -\frac{W\tan(\theta)g(W\tan(\theta))(2\phi(W)-1)}{\sigma^2},$$

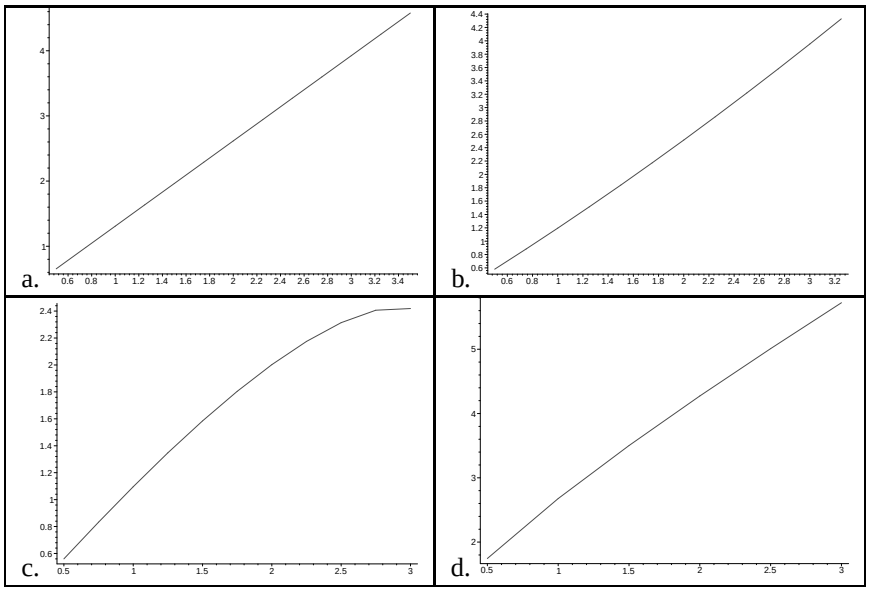

Table 2: Extrema position as a function of the scale.
a) Constant intensity variation ($A_1 - A_0 = 10, \theta_1 = \frac{\pi}{3}$ and $\theta_0 = -\frac{\pi}{3}$). b) Linear intensity variation ($K = 0.1$) . c) Nonlinear intensity variation ($K = 0.05$). d) Curved edges ($K = 0.2$).

$$\nabla^2 F(W,0) = -\frac{W\sin(\theta)g(\sin(\theta))(2(\phi(W\cos(\theta)) - \phi(W\frac{\sin^2(\theta)}{\cos(\theta)})) - 2)}{\sigma^2},$$

and

$$\nabla^2 F(W, W\tan(\theta)) = -\frac{Wg(W)(2\phi(W\tan(\theta)) - 1)}{\sigma^2}.$$

For both models extrema points are provided inside the corner sectors (see figure 2 and 5). They move in scale space away from the corner and at a high scale, we can remark that only one extremum remains (see figure 3 and 7). We can remark that either the model is symmetric and then the extrema merge or the model is not symmetric and then only one extremum remains at a high scale.

Moreover, the Laplacian at the corner point is different from zero for each model. However when the size of the filter is small compared to the model *i.e.* $W \to \infty$ or $\sigma \to 0$ then we can easily show (using the property: $x \to \infty$, $-x^a e^{-cx^b} \to 0$ when $a = 0$ or 1 and $b, c > 0$ and the property: $\forall\, x \;\; 0 < \phi(x) < 1$) that the value at each corner points approaches zero. Figure 6 shows the numerical position of the zero-crossings at a low scale and at a high one. At a low scale we can remark that the zero-crossings go through the corner points.

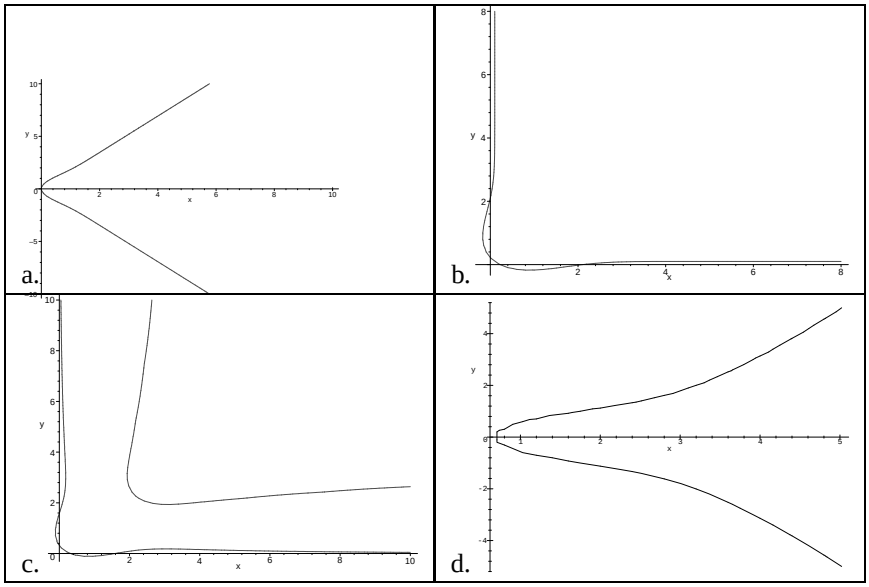

Table 3: Zero-crossings contour.
a) Constant intensity variation ($A_1 - A_0 = 10, \theta_1 = \frac{\pi}{3}$ and $\theta_0 = -\frac{\pi}{3}$). b) Linear intensity variation ($K = 0.1$) . c) Nonlinear intensity variation ($K = 0.05$). d) Curved edges ($K = 0.2$).

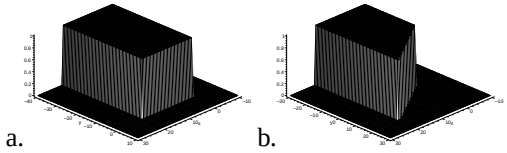

Figure 1: Infinite multi-model for $W = 20$.
a) $\theta = 0$. b) $\theta = \frac{\pi}{4}$.

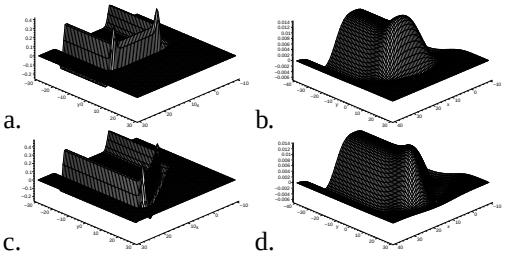

Figure 2: Laplacian of Gaussian for the infinite multi-models at two scales ($\sigma = 1$ and $\sigma = 5$).
a) and b) $\theta = 0$. c) and d) $\theta = \frac{\pi}{4}$.

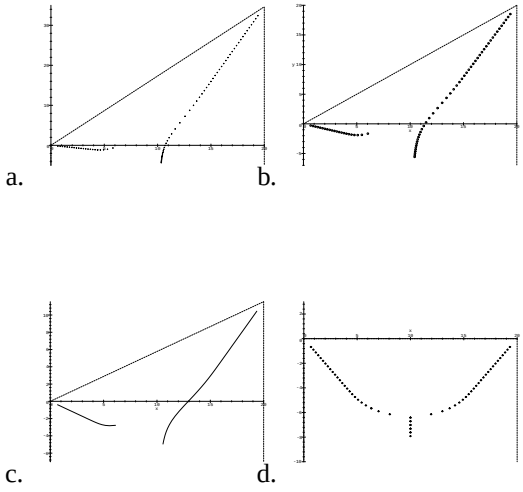

Figure 3: Behavior of extrema in scale space for an infinite multi-model ($W = 20$). *a), b), c) and d)* $\theta = \frac{\pi}{3}, \frac{\pi}{4}, \frac{\pi}{6}$ *and* 0. *In each case the 2D intensity models (dashed lines) are superimposed on the behavior of the extrema.*

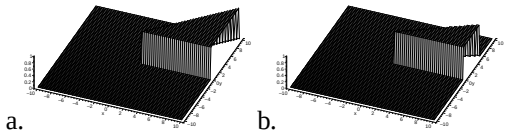

Figure 4: A closed multi-model.
a) and b) Example of $3D$ *model for* $W = 10$ *and* $\theta = \frac{\pi}{4}$ *and* $\frac{\pi}{6}$.

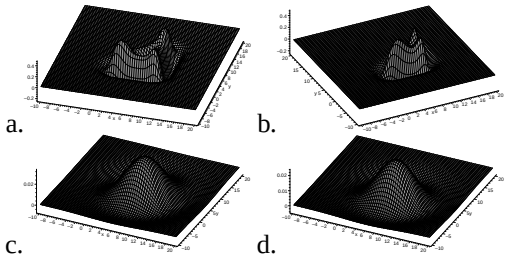

Figure 5: Laplacian of Gaussian for the closed multi-model at two scales $\sigma = 1$ and $\sigma = 5$.
a) and c) $\theta = \frac{\pi}{4}$. *b) and d)* $\theta = \frac{\pi}{6}$.

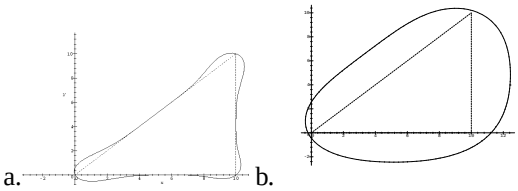

Figure 6: Zero-crossings contour of the closed multi-model for $\sigma = 1$ and $\sigma = 3$. *The 2D intensity model (dashed lines) is superposed on the zero-crossings contour.*

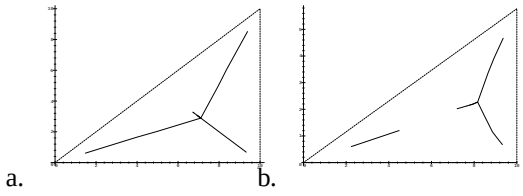

Figure 7: Behavior of the extrema for the closed multi-model. *a)* $\theta = \frac{\pi}{4}$. *b)* $\theta = \frac{\pi}{6}$.

0.7 Other junction models

In this section, we consider models that are defined as the intersection of several regions (greater than 2). Corners detectors often fail in detecting this kinds of junction which are also relevant features in computer vision. Our aim is to show that extrema points are also provided for these models inside the junction sectors.

0.7.1 Definitions

- **Trihedral junction model**

  For this model let (see figure 8) :

  $$I(x,y) = A_0 + (A_1 - A_0) \times H(ycos(\theta_0) - x\sin(\theta_0)) \times H(x\sin(\theta_1) - y\cos(\theta_1)) +$$
  $$(A_2 - A_1) \times H(y\cos(\theta_1) - x\sin(\theta_1)) \times H(x\sin(\theta_2) - y\cos(\theta_2)).$$

  As the L-junction model with constant intensity (see §3) :

  $$\nabla^2 F(x,y) = \frac{1}{\sigma^2} \sum_{i=0}^{2} (A_i - A_{((i+1) \bmod 3)}) u_i g(u_i) \phi(v_i), \qquad (3)$$

  where u_i and v_i are defined in section 3.

- **X-junction model**

  For this model, let:

  $$I(x,y) = A_0 + (A_1 - A_0) \times H(y\cos(\theta_0) - x\sin(\theta_0)) \times H(x\sin(\theta_1) - y\cos(\theta_1)) + (A_2 - A_1) \times$$
  $$H(y\cos(\theta_1) - x\sin(\theta_1)) \times H(x\sin(\theta_2) - y\cos(\theta_2)) + (A_3 - A_2) \times$$
  $$H(y\cos(\theta_2) - x\sin(\theta_2)) \times H(x\sin(\theta_3) - y\cos(\theta_3))$$

  and :

  $$\nabla^2 F(x,y) = \frac{1}{\sigma^2} \sum_{i=0}^{3} (A_i - A_{((i+1) \bmod 4)}) u_i g(u_i) \phi(v_i) \qquad (4)$$

For both models we can see that one or several extrema are located inside the junction sectors (see figure 9 and 13). The number of extrema depends on the configuration. When the polarity of the Laplacian response along the junction contour is the same we find an extremum inside the corresponding sector if this one is sharp. Figure 10 shows the only two possible configurations encountered for the trihedral junction model. For example, figure 9.a is a consequence of the configuration of figure 10.b and figure 9.b of figure 10.a. For the X-junction model, the number of extrema is either two or four (see fig. 12 and 13). As for the corner model the position of the extremum depends on the scale and the sector aperture. Numerical positions of the extrema as a function of the scale and the sector aperture are shown on figure 11.

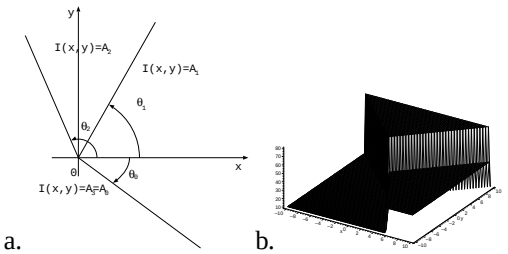

Figure 8: Y-junction model.
a) 2D model. b) Example of 3D model for $A_1 = 30, A_2 = 50, A_3 = 60\, \theta_0 = -\frac{\pi}{3}, \theta_1 = \frac{\pi}{4}, \theta_2 = 3\frac{\pi}{4}$.

Furthermore, we can easily prove that the responses for the two models at the junction points are zero. We can generalize this property to an n-ary junction model defined as the intersection point of n surface sectors with constant intensities A_i and aperture $\theta_{i+1} - \theta_i$. Let I_n be an n-ary junction:

$$I_n(x,y) = A_0 + \sum_{i=0}^{n} (A_{(((i+1) \bmod (n+1))} - A_i) H(\sin(\theta_{i+1})x - \cos(\theta_{i+1})y) H(\cos(\theta_i)y - \sin(\theta_i)x),$$

where $\theta_{i+1} > \theta_i$. The filtered image is given by:

$$F(x,y) = \int_{-\infty}^{\infty} \int_{-\infty}^{\infty} A_0 + \sum_{i=0}^{n} (A_{(((i+1) \bmod (n+1))} - A_i) \times$$

$$H(\sin(\theta_{i+1})(x-\alpha) - y(\cos(\theta_{i+1}) - \beta)) H(\cos(\theta_i)(y-\beta) - \sin(\theta_i)(x-\alpha)) g(\alpha) g(\beta) d\alpha d\beta.$$

The response of the Laplacian of Gaussian detector to a general n-ary junction is:

$$\nabla^2 F(x,y) = \frac{1}{\sigma^2} \sum_{i=0}^{n} (A_i - A_{(((i+1) \bmod (n+1))}) u_i g(u_i) \phi(v_i) \tag{5}$$

with $A_0 = A_{n+1}, \theta_i < \theta_{i+1}$ and $n \geq 1$. We have the following property:

$$\nabla^2 F(0,0) = 0. \tag{6}$$

That is, the Laplacian of Gaussian is zero for any junction point with an infinite extent model and a constant illumination. As the Laplacian of a general n-ary junction is defined by a summation and due to the polarity of the response along the contour, the following conjecture is set:

Conjecture 1 *When the number of sectors* n_s *(*$n_s > 2$*) is:*

- *even: the number of extrema varies from* 2 *up to* n_s
- *odd: the number of extrema varies from* 1 *up to* $n_s - 1$

For example, on the Figure 14 we have shown the two extrema configurations limit for a 8-ary junction. That is, 2 (see figure 14.a and b) and 8 extrema (see figure 14.c and d).

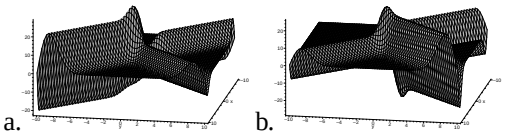

Figure 9: Laplacian of Gaussian for the Y-junction model.
$\theta_0 = -\frac{\pi}{4}, \theta_1 = \frac{\pi}{4}$ *and* $\theta_2 = \frac{3\pi}{4}$. *a)* 3*D surface with one extremum for* $A_1 = 100$, $A_2 = 60$ *and* $A_3 = 10$, *b)* 3*D surface with two extrema for* $A_1 = 100$, $A_2 = 10$ *and* $A_3 = 60$.

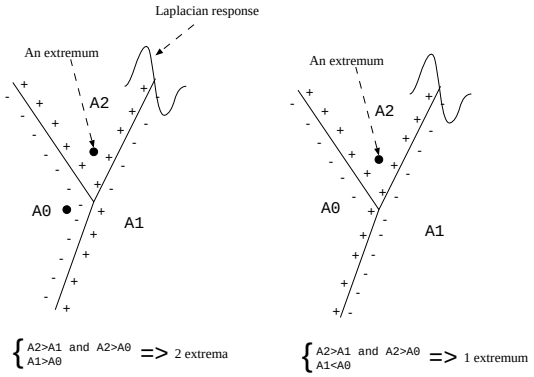

Figure 10: Number of extrema for an Y-junction model.

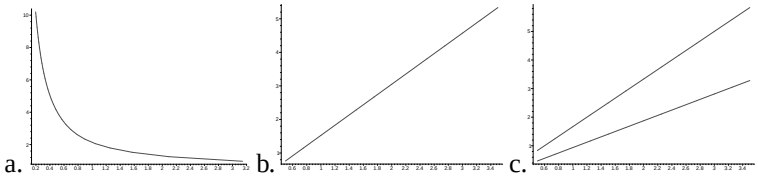

Figure 11: Behavior of the extrema for an Y-junction model.
a) Behavior of the extremum value as a function of the sector aperture in the bisector direction $\theta_1 - \theta_0 = \frac{2\pi}{i}$, $i = 2..32$. *b) Behavior of the extremum position as a function of the scale for the model of figure 9.a. c) Behavior of the two extrema position as a function of the scale for the model of figure 9.b.*

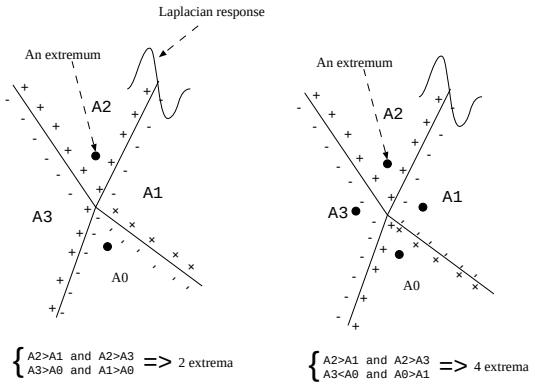

Figure 12: Number of extrema for the X-model.

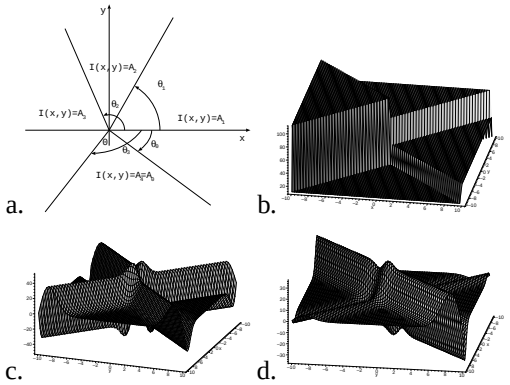

Figure 13: Laplacian of Gaussian for the X-junction model.
a) and b) Example of 2*D and* 3*D models. c)* 3*D surface with four extrema for* $A_1 = 10, A_2 = 160, A_3 = 30, A_0 = 140, \theta_0 = -\frac{\pi}{4}, \theta_1 = \frac{\pi}{4}, \theta_2 = 3\frac{\pi}{4}$ *and* $\theta_3 = -\frac{3\pi}{4}$*. c)* 3*D surface with two extrema using the same previous parameters except for* $A_1 = 140$ *and* $A_0 = 10$*.*

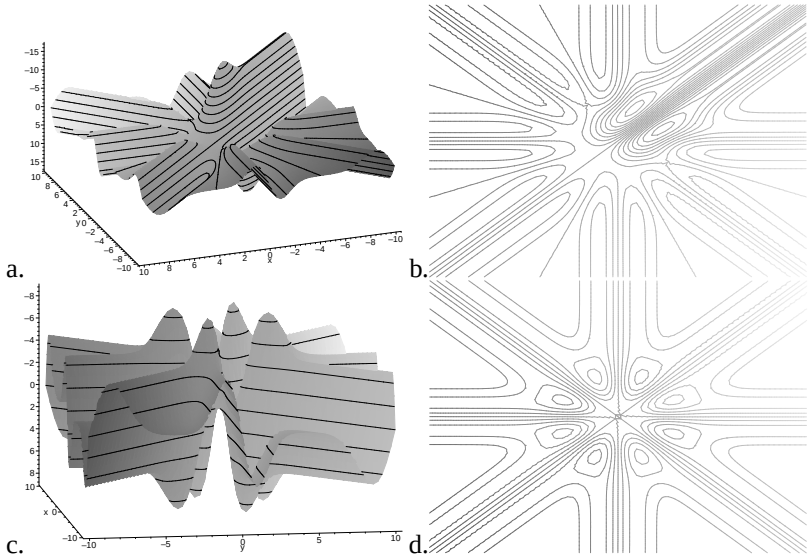

Figure 14: Laplacian of Gaussian for a model with 8 sectors.
In both cases $\sigma = 1$ *and* $\theta_0 = -\pi, \theta_1 = -\frac{3\pi}{4}, \theta_2 = -\frac{\pi}{2}, \theta_3 = -\frac{\pi}{4}, \theta_4 = 0, \theta_5 = \frac{\pi}{4}, \theta_6 = \frac{\pi}{2}, \theta_7 = \frac{3\pi}{4}$. *a) and b) The responses and the level sets for* $A_0 = 10, A_1 = 30, A_2 = 50, A_3 = 70, A_4 = 90, A_5 = 110, A_6 = 130, A_7 = 150$. *c) and d) The responses and the level sets for* $A_0 = 10, A_1 = 30, A_2 = 10, A_3 = 30, A_4 = 10, A_5 = 30, A_6 = 10, A_7 = 30$.

0.8 Conclusion

We have shown that the Laplacian of Gaussian of all the junction models studied in this paper provide one or several extrema inside the junction sector. These extrema have nice scaling properties. When a same model is rotated or scaled or the variation of illumination is modified, an extremum is always provided inside the corner sector. Furthermore, if the model is symmetric (always true for L-junction), the gradient orientation for every point on the corner bisector is equal to the angle between the corner bisector and the x-axis. The importance of defining a framework for evaluating and comparing different interest point detectors has been pointed out in [19]. The main criterion presented concerns the stability of the detector under geometric transformations. The extrema points can be reliable starting points for detecting junction points, for tracking or indexing images.

Furthermore we have seen that under some conditions the Laplacian is not zero at the junction point:

- for linear models (n-ary junction models: L, Y, X,...) with constant illumination, the Laplacian of Gaussian is zero at the junction point,
- for linear models with non-constant illumination and infinite extent, the Laplacian is not zero at the junction points and its value depends on the illumination variation,
- for nonlinear models with constant illumination and infinite extent the Laplacian is not zero at the junction points and its value depends on the model curvature,
- for closed models, the Laplacian is not zero at the junction points and it tends to zero when the size of the model is wide compared to the size of the filter.

Therefore we conclude that approaches based on the Laplacian of the Gaussian to detect corners are not appropriate (linear models with constant illumination are unusual in gray scale images). We believe, due to the complexity of the physical phenomenon underlying the image formation, that the junction must be, for greater precision, detected on the gray scale image.

0.9 Acknowledgements

All the drawings and the numerical approximation inside this paper were made by Maple 4 ©.

0.10 Appendix A

$$\begin{aligned} F(x,y) &= (G * I)(x,y) = \int_{-\infty}^{\infty}\int_{-\infty}^{\infty} I(x-\epsilon, y-\eta)G(\epsilon,\eta)\,d\eta\,d\epsilon \\ &= (A_1 - A_0)\int_{\epsilon=-\infty}^{x}\int_{\eta=y-(x-\epsilon)\tan\theta_1}^{y-(x-\epsilon)\tan\theta_0} G(\epsilon,\eta)\,d\eta\,d\epsilon + A_0 \end{aligned}$$

$$= \quad (A_1 - A_0)(F^{\theta_0}(x,y) - F^{\theta_1}(x,y)) + A_0$$

with $F^\theta(x,y) = \int_{\epsilon=-\infty}^{x} \int_{\eta=0}^{y-(x-\epsilon)\tan\theta} G(\epsilon,\eta)d\eta d\epsilon = \int_{\epsilon=-\infty}^{x} g(\epsilon)(\Phi(y-(x-\epsilon)\tan\theta) - \frac{1}{2})d\epsilon$.

We have :

$$\begin{aligned}
F_y^\theta(x,y) &= \int_{\epsilon=-\infty}^{x} G(\epsilon, y-(x-\epsilon)\tan\theta)d\epsilon \\
&= \int_{\epsilon=-\infty}^{x} G(\cos\theta(y - x\ \tan\theta), \frac{\epsilon}{\cos\theta} + \sin\theta(y - x\ \tan\theta))d\epsilon \\
&= \cos\theta g(\cos\theta y - \sin\theta x) \int_{\epsilon=-\infty}^{\frac{x}{\cos\theta}} g(\epsilon + \sin\theta(y - x\ \tan\theta))d\epsilon \\
&= \cos\theta g(\cos\theta y - \sin\theta x)[\phi(\epsilon + \sin\theta(y - x\ \tan\theta))]_{-\infty}^{\epsilon=\frac{x}{\cos\theta}} \\
&= \cos\theta g(\cos\theta y - \sin\theta x)\phi(\cos\theta\, x + \sin\theta y)
\end{aligned}$$

Similarly, we have :

$$\begin{aligned}
F_x^\theta(x,y) &= -\tan\theta \int_{\epsilon=-\infty}^{x} G(\epsilon, y-(x-\epsilon)\tan\theta)d\epsilon \\
&\quad + \int_{\eta=0}^{y} G(x,\eta)d\eta \\
&= -\sin\theta g(\cos\theta y - \sin\theta x)\phi(\cos\theta\, x + \sin\theta y) \\
&\quad + g(x)\left(\phi(y) - \frac{1}{2}\right)
\end{aligned}$$

Therefore :

$$\begin{aligned}
F_x(x,y) &= (A_0 - A_1)\sin\theta_0 g(\cos\theta_0 y - \sin\theta_0 x)\phi(\cos\theta_0\, x + \sin\theta_0 y) \\
&\quad + (A_1 - A_0)\sin\theta_1 g(\cos\theta_1 y - \sin\theta_1 x)\phi(\cos\theta_1\, x + \sin\theta_1 y)
\end{aligned}$$

and

$$\begin{aligned}
F_y(x,y) &= (A_1 - A_0)\cos\theta_0 g(\cos\theta_0 y - \sin\theta_0 x)\phi(\cos\theta_0\, x + \sin\theta_0 y) \\
&\quad + (A_0 - A_1)\cos\theta_1 g(\cos\theta_1 y - \sin\theta_1 x)\phi(\cos\theta_1\, x + \sin\theta_1 y)
\end{aligned}$$

0.11 Appendix B

We will study in the following appendix the extrema points and the hyperbolic points of $\nabla^2 F$. More precisely, we will prove that $\nabla^2 F$ has only one hyperbolic point and one extremum point which lie on the bisector line. This study will be decomposed in three parts :

- in the first part, we will introduce basic notations and propositions,

- in the second part, we show that these points are on the bisector line, and we look for all the values which corresponds to a extremum point or a hyperbolic point when θ goes in $]0, \frac{\pi}{2}[$,
- in the third part, we look for the properties of the extrema or hyperbolic points of $\nabla^2 F$ in all the plane, and we show that theses properties imply that these points lie only on the bisector line.

Basic considerations

As Formula 1 is independent by rotation, we can take $\theta_1 = -\theta_0 = \theta$, we obtain :

$$\nabla^2 F(x,y) = \frac{A_1 - A_0}{\sigma^2} \left(u_1 g(u_1)\Phi(v_1) - u_0 g(u_0)\Phi(v_0)\right),$$

with $u_1 = y\,\cos\theta - x\,\sin\theta$, $u_0 = y\,\cos\theta + x\,\sin\theta$, $v_1 = x\,\cos\theta + y\,\sin\theta$, $v_0 = x\,\cos\theta - y\,\sin\theta$.

In the following, we will note :

- $X = \frac{x}{\sigma}, Y = \frac{y}{\sigma}$,
- $g_1(x) = \frac{1}{\sqrt{2\pi}} e^{-\frac{x^2}{2}}$,
- $\Phi_1(x) = \int_{-\infty}^{x} g_1(t)dt$,
- $J(x) = \frac{g_1(x)}{\Phi_1(x)}$,
- $U_i = \frac{u_i}{\sigma}, V_i = \frac{v_i}{\sigma}$ for $i \in [0,1]$,
- $G(X,Y) = (U_1 g_1(U_1)\Phi_1(V_1) - U_0\, g_1(U_0)\Phi_1(V_0))$.

We have the following proposition :

Proposition 3

$$\nabla^2 F(x,y) = \frac{A_1 - A_0}{\sigma^2} G(X,Y).$$

Proof :

Indeed we have $g(u_i) = \frac{1}{\sigma} g_1(U_i)$ and $\Phi(v_i) = \Phi(V_i)$ and so

$$\nabla^2 F(x,y) = \frac{A_1 - A_0}{\sigma^2} \left(U_1 g_1(U_1)\Phi_1(V_1) - U_0 g_1(U_0)\Phi_1(V_0)\right).$$

□

This means that we can study the function $G(X,Y)$ to get the extrema of $\nabla^2 F(x,y)$ when σ are fixed (by multiplying the resulting values by σ).

In the following, we need to surround $J(x)$ and we use the value γ_0 which will appear very often, in this appendix :

Proposition 4

- *When* $x < 0$ *then* $\frac{-x+\sqrt{x^2+\frac{8}{\pi}}}{2} \leq J(x) \leq \frac{-x+\sqrt{x^2+4}}{2}$,
- *Let* $f(x) = \Phi_1(x) + x\, g_1(x)$. *Then* $f(x) > 0$ *if and only if* $x > \gamma_0$ *where* γ_0 *is the only root of* $f(x) = 0$. *Moreover, we have* $-1 < -\sqrt{\frac{2}{3}} < \gamma_0 < -\frac{\sqrt{2}}{2} < 0$.

Proof :

Using the approximation given for the Erf function in the Encyclopedia of Mathematic [27] with $e^{x^2} = \frac{1}{\sqrt{2\pi}\, g(-\sqrt{2}x)}$, $\int_x^\infty e^{-t^2} dt = \frac{\Phi_1(-\sqrt{2}x)}{\sqrt{\pi}}$, we get :

$$\frac{1}{x+\sqrt{x^2+2}} < \frac{1}{\sqrt{2}\, J(-\sqrt{2}x)} < \frac{1}{x+\sqrt{x^2+\frac{4}{\pi}}}$$

and with $u = -x\sqrt{2}$,

$$\frac{-u+\sqrt{u^2+\frac{8}{\pi}}}{2} < J(u) < \frac{-u+\sqrt{u^2+4}}{2}.$$

This ends the first part of the proof.

Now we get $f'(x) = g_1(x)(1+(1-x^2))$. Therefore f is decreasing when $|x| \geq \sqrt{2}$ and increasing when $-\sqrt{2} \leq x \leq \sqrt{2}$. However we have $\lim_{-\infty} f = 0$ and $\lim_{\infty} f = 1$. Therefore f has only one root γ_0 which is greater than $-\sqrt{2}$ and is positive when $x > \gamma_0$ (resp. negative when $x < \gamma_0$).

It remains to prove that $-\sqrt{\frac{2}{3}} < \gamma_0 < -\frac{\sqrt{2}}{2}$ which is equivalent to prove that $f(-\sqrt{\frac{2}{3}}) < 0$ and $f(-\frac{\sqrt{2}}{2}) > 0$.

Indeed, we have $f(-\sqrt{\frac{2}{3}}) = g_1(-\sqrt{\frac{2}{3}}) \left(\frac{\Phi_1(-\sqrt{\frac{2}{3}})}{g_1(-\sqrt{\frac{2}{3}})} - \sqrt{\frac{2}{3}} \right)$. But using the previous lower-bound, we find $\frac{\Phi_1(-\sqrt{\frac{2}{3}})}{g_1(-\sqrt{\frac{2}{3}})} - \sqrt{\frac{2}{3}} \leq \frac{2}{\sqrt{\frac{2}{3}}+\sqrt{\frac{2}{3}+\frac{8}{\pi}}} - \sqrt{\frac{2}{3}} < 0$.

Similarly, using the previous upper-bound, we get $\frac{\Phi_1(-\frac{\sqrt{2}}{2})}{g_1(-\frac{\sqrt{2}}{2})} - \frac{\sqrt{2}}{2} > \frac{2}{\frac{\sqrt{2}}{2}+\sqrt{\frac{1}{2}+4}} - \frac{\sqrt{2}}{2} = 0$, and $f(-\frac{\sqrt{2}}{2}) > 0$.

This ends the proof.

□

Behavior of $\nabla^2 F$ on the straight line $y = 0$

Let note $h(x) = \Phi_1(x\, \cos\theta) + \frac{x\, \cos\theta\, g_1(x\, \cos\theta)}{1-x^2\, \sin^2\theta}$.

Theorem 1 $\frac{\delta G(X,Y)}{\delta X}(X,0)$ *has two zeroes* X_0 *and* X_1 *which verify the following conditions :*

- *they are the two unique zeroes of* h,
- $h(X_0) = h(X_1) = 0$,
- $-\frac{\sqrt{3-\sqrt{9-8\, \sin^2\theta}}}{\sqrt{2}\sin\theta} < X_0 < 0$,

- $\frac{1}{\sin\theta} < X_1 < \frac{\sqrt{3+\sqrt{9-8\ \sin^2\theta}}}{\sqrt{2}\sin\theta}$,
- $\frac{\delta^2 G(X,Y)}{\delta X \delta X}(X_0, 0) < 0$, $\frac{\delta^2 G(X,Y)}{\delta X \delta X}(X_1, 0) > 0$,

Proof :

By derivation, we have :

$$\frac{\delta G(X,Y)}{\delta X}(X, 0) = -2\ \sin\theta g_1(X\ \sin\theta)\left((1-\sin^2\theta X^2)\Phi_1(X\ \cos\theta) + \cos\theta\, X\, g_1(X\ \cos\theta)\right).$$

Let note $i(x) = \sin^2\theta X^2 - 1$, we have $\frac{\delta G(X,Y)}{\delta X}(X, 0) = 2\ \sin\theta g_1(X\ \sin\theta) i(X)\, h(X)$.
As $\frac{\delta G(X,Y)}{\delta X}(\frac{1}{\sin\theta}, 0) = -2\cos\theta\, g_1(1)\, g_1(\frac{\cos\theta}{\sin\theta}) \neq 0$ and similarly $\frac{\delta G(X,Y)}{\delta X}(-\frac{1}{\sin\theta}, 0) \neq 0$, the zeroes of $\frac{\delta G(X,Y)}{\delta X}(X, 0)$ are also the zeroes of h.
In order to find the zeroes of h, we compute the derivated of h :

$$\begin{aligned} h'(x) &= \cos\theta\, g_1(x\ \cos\theta)\left(1 + \frac{(1-\cos^2\theta\, x^2)(1-\sin^2\theta x^2) + 2\ \sin^2\theta x^2}{(1-\sin^2\theta x^2)^2}\right) \\ &= \frac{\cos\theta\, g_1(x\ \cos\theta)}{(1-\sin^2\theta x^2)^2}\left(2 - x^2 + \sin^2\theta\, x^4\right) \\ &= \frac{\cos\theta\, g_1(x\ \cos\theta)}{(1-\sin^2\theta x^2)^2} k(x) \end{aligned}$$

where $k(x) = 2 - x^2 + \sin^2\theta\, x^4$.
Two cases can appear :

- When $1 \leq 8\ \sin^2\theta$
  In this case, $k(x)$ is always positif. Therefore $h(x)$ is increasing in x in $]-\infty, -\frac{1}{\sin\theta}[$, $]-\frac{1}{\sin\theta}, \frac{1}{\sin\theta}[$ and $]-\frac{1}{\sin\theta}, \infty[$. Using $\lim_{x\to-\infty} h(x) = 0$ and $\lim_{x\to\infty} h(x) = 1$, $h(0) = \frac{1}{2}$. There exists X_0, X_1 (with $-\frac{1}{\sin\theta} < X_0 < 0$ and $\frac{1}{\sin\theta} < X_1$) such that $h(X_0) = h(X_1) = 0$.
  Moreover, we have $\frac{\delta^2 G(X,Y)}{\delta X \delta X}(X_0, 0) < 0$ and $\frac{\delta^2 G(X,Y)}{\delta X \delta X}(X_1, 0) > 0$.
- When $1 > 8\ \sin^2\theta$
  In this case, $k(x) = 0$ has four roots in x : $-\alpha_1, -\alpha_0, \alpha_0, \alpha_1$ with $\alpha_0 = \frac{\sqrt{1-\sqrt{1-8\ \sin^2\theta}}}{\sqrt{2}\sin\theta}$ and $\alpha_1 = \frac{\sqrt{1+\sqrt{1-8\ \sin^2\theta}}}{\sqrt{2}\sin\theta}$.
  As $0 < \alpha_0 < \frac{1}{\sqrt{2}\sin\theta} < \alpha_1 < \frac{1}{\sin\theta}$ and $h(\alpha_0) > 0$, $h(\alpha_1) > 0$, $\lim_{x\to-\infty} h(x) = 0$ and $\lim_{x\to\infty} h(x) = 1$, h increases in:
  - $]-\infty, -\frac{1}{\sin\theta}[$ from 0 up to ∞,
  - $]-\frac{1}{\sin\theta}, -\alpha_1]$ from $-\infty$ up to $h(-\alpha_1)$,
  - $[-\alpha_0, \alpha_0]$ up to $h(\alpha_0) > 0$ (clearly a sum of positive terms),
  - $[\alpha_1, \frac{1}{\sin\theta}[$ up to ∞,
  - $]\frac{1}{\sin\theta}, \infty]$ from $-\infty$ to 1.

  and h decreases in:
  - $[-\alpha_1, -\alpha_0]$ down to $h(-\alpha_0)$,
  - $[\alpha_0, \alpha_1]$ down to $h(\alpha_1) > 0$(clearly a sum of positive terms).

Now, in order to find the number of zeroes of h, we need first to show the following lemma :

Lemma 1 $h(-\alpha_1) < 0$.

Proof :

Indeed, we have

$$h(-\alpha_1) = \Phi_1(-\alpha_1 \cos\theta) - \frac{\cos\theta\alpha_1^3}{2} g_1(\alpha_1 \cos\theta)$$

and

$$\frac{\delta h(-\alpha_1)}{\delta\theta} = -\frac{g(\alpha_1\cos\theta)}{4\alpha_1 \sin^7\theta}\left(Z(1-4\sin^2\theta)+1-8\cos^2\theta\sin^2\theta\right)$$

with $Z = \sqrt{1-8\sin^2\theta}$.
Since $1-4\sin^2\theta > 0$ and $1-8\cos^2\theta\sin^2\theta > 0$, $\frac{\delta h(-\alpha_1)}{\delta\theta} < 0$.
So $h(-\alpha_1)$ is decreasing, but when θ goes down to 0, $\lim\alpha_1 = \infty$, and $\lim h(-\alpha_1) = 0$. Therefore $h(-\alpha 1)$ is always negative.

□

Therefore, in this case, there exists two values X_0, X_1 (with $-\frac{1}{\sin\theta} < X_0 < 0$ and $\frac{1}{\sin\theta} < X_1$) such that $h(X_0) = h(X_1) = 0$.

Moreover, we have $\frac{\delta^2 G(X,Y)}{\delta X \delta X}(X_0, 0) < 0$, $\frac{\delta^2 G(X,Y)}{\delta X \delta X}(X_1, 0) > 0$.

Let note $\beta_0 = \frac{\sqrt{3-\sqrt{9-8\sin^2\theta}}}{\sqrt{2}\sin\theta}$ and $\beta_1 = \frac{\sqrt{3+\sqrt{9-8\sin^2\theta}}}{\sqrt{2}\sin\theta}$.
There remains to prove that $-\beta_0 < X_0$ and $X_1 < \beta_1$.
But noting that $-\frac{1}{\sin\theta} < -\beta < 0$ and $\frac{1}{\sin\theta} < \beta_1$, we will prove in the following that $h(-\beta_0) < 0$ and $h(\beta_1) > 0$, using the variation of h, this will end the proof.
Indeed, we have :

$$\frac{\delta h(\frac{\sqrt{3+\sqrt{9-8\sin^2\theta}}}{\sqrt{2}\sin\theta})}{\delta\theta} = \frac{2\cos^2\theta g_1(\cos\theta\beta_1)\left(Z(4+5\cos^2\theta)+4\cos^4\theta+19\cos^2\theta+4\right)}{Z\beta_1\sin^5\theta(1-\sin\theta^2\beta_1^2)^3}$$

with $Z = \sqrt{9-8\sin^2\theta}$. Since $1-\sin\theta^2\beta_1^2 < 0$, we get $\frac{\delta h(\beta_1)}{\delta\theta} < 0$ and using $h(\beta_1) \geq h_{\theta=\frac{\pi}{2}}(\beta_1) = \Phi_1(1) > 0$.
Similarly we have :

$$\frac{\delta h(-\beta_0)}{\delta\theta} = \frac{2\cos^2\theta g_1(\cos\theta\beta_0)\left(-Z(4+5\cos^2\theta)+4\cos^4\theta+19\cos^2\theta+4\right)}{Z\beta_0\sin^5\theta(1-\sin\theta^2\beta_0^2)^3}$$

But since $1-\sin\theta^2\beta_0^2 > 0$ and $-Z(4+5\cos^2\theta)+4\cos^4\theta+19\cos^4\theta+4 < 0$, $\frac{\delta h(-\beta_0)}{\delta\theta} < 0$, we get $\frac{\delta h(-\beta_0)}{\delta\theta} < 0$, $h(-\beta_0) < h_{\theta=0}(0) = 0$.

□

Theorem 2 *We have :*

- $\frac{\delta G(X,Y)}{\delta Y}(X, 0) = 0$ *for all values of* X,
- $\frac{\delta^2 G(X,Y)}{\delta Y \delta Y}(X_0, 0) > 0$,

- $\frac{\delta^2 G(X,Y)}{\delta Y \delta Y}(X_1, 0) > 0.$

Proof :

For reason of the symmetry of the problem, we have $G(X, Y) = G(X, -Y)$ and $\frac{\delta G(X,Y)}{\delta Y}(X, 0) = 0$.

Now, we want to study the sign of $\frac{\delta^2 G(X,Y)}{\delta Y \delta Y}(X, 0)$ in $X = X_0$ and $X = X_1$.

Using

$$\frac{\delta^2 G(X,Y)}{\delta Y \delta Y}(X, 0) = 2 \cos\theta \sin\theta \, g_1(X \sin\theta) l(X)$$

with $l(x) = \cos\theta \, X(3 - \sin^2\theta \, X^2)\Phi_1(X \cos\theta) + (2 - \sin^2\theta \, X^2) g_1(X \cos\theta)$ and

$$\Phi_1(X \cos\theta) = -\frac{\cos\theta \, X \, g_1(X \cos\theta)}{1 - \sin^2\theta X^2}$$

when $X = X_0$ or X_1 (see Theorem 1), we get in these two cases :

$$l(x) = \frac{2 - 3\,x^2 + \sin^2\theta \, x^4}{1 - \sin^2\theta x^2} g_1(x \cos\theta).$$

But, $l(x) = 0$ has four roots in $x : \pm\frac{\sqrt{3 - \sqrt{9 - 8 \sin^2\theta}}}{\sqrt{2}\sin\theta}$ and $\pm\frac{\sqrt{3 + \sqrt{9 - 8 \sin^2\theta}}}{\sqrt{2}\sin\theta}$.

Using $-\frac{\sqrt{3 - \sqrt{9 - 8 \sin^2\theta}}}{\sqrt{2}\sin\theta} < X_0 < 0$ and $\frac{1}{\sin\theta} < X_1 < \frac{\sqrt{3 + \sqrt{9 - 8 \sin^2\theta}}}{\sqrt{2}\sin\theta}$ (see Theorem 1), we get easily $l(X_0) > 0$ and $l(X_1) > 0$. This ends the proof.

□

We will prove in the next section that the extremum or hyperbolic points of $G(X, Y)$ are on the straight line $Y = 0$. In order to prove that we will need to know the location of the X values which corresponds to these points on the line $Y = 0$ this is the aim of the next theorem.

Theorem 3 *When θ varies in $]0, \frac{\pi}{2}[$, $h(X) = 0$ has one and only one solution when $-1 < X < \gamma_0$ and $1 < X$.*

Proof :

Indeed, we have :

$$\frac{\delta h(X)}{\delta\theta} = \frac{V \, g_1(X \cos\theta)}{(1 - V^2)^2}(-2 + 3\,X^2 - X^2\,V^2)$$

with $V = X \sin\theta$ and we have when $\theta = \frac{\pi}{2}$, $h(X) = \frac{1}{2} > 0$.

We can remark that $0 < V \leq X$ if $X \geq 0$ (respectively $X \leq V < 0$, if $X < 0$), and that $-2 + 3\,X^2 - X^2\,V^2$ has :

- no zero if $|X| < \sqrt{\frac{2}{3}}$,
- one positive zero which is less or equal than 1 (resp. negative and smaller or equal to -1) if $\sqrt{\frac{2}{3}} < |X| \leq 1$,
- one positive zero which is greater than 1 (resp. negative and smaller than -1) if $1 < |X|$.

So we will subdivide the proof in many cases.

- when $X \leq -1$ or $0 \leq X < \sqrt{\frac{2}{3}}$ or $\sqrt{\frac{2}{3}} \leq X \leq 1$,

  by noting that $-1 < -\frac{\sqrt{3-\sqrt{9-8\,\sin^2\theta}}}{\sqrt{2}\sin\theta}$, Theorem 1 implies that $h(X)$ has no zero in these cases.

- when $1 < X$:
  In this case, $h(X)$ is increasing between 0 and θ_0 (with $\theta_0 = \arcsin\left(\frac{1}{X}\right)$) and between θ_0 and $min(\frac{\pi}{2}, \theta_1)$ (with $\theta_1 = \arcsin\left(\frac{\sqrt{3\,X^2-2}}{X^2}\right)$). If $\theta_1 > \frac{\pi}{2}$, $h(X)$ is decreasing between θ_1 and $\frac{\pi}{2}$.
  Using $h_{\theta=\frac{\pi}{2}}(X) > 0$, $h_{\theta=0}(X) = \Phi_1(X) + X\,g_1(X) > 0$, $\lim_{X\to\theta_0-} h(X) = +\infty$, $\lim_{X\to\theta_0+} h(X) = -\infty$, $h(X)$ has always an unique zero.

- when $-\sqrt{\frac{2}{3}} < X \leq 0$:
  In this case $h'(X)$ is increasing in θ. We have $h_{\theta=\frac{\pi}{2}}(X) > 0$ and $h_{\theta=0}(X) = \Phi_1(X) + X\,g_1(X)$.
  Therefore using Proposition 4, we find a zero of $h(X)$ only if $-\sqrt{\frac{2}{3}} < X < \gamma_0$ (the case $X = \gamma_0$ corresponds to $\theta = 0$ so we exclude it).

- when $-1 < X \leq -\sqrt{\frac{2}{3}}$:
  In this case, $h(X)$ is decreasing between 0 and θ_0 and increasing between θ_0 and $\frac{\pi}{2}$ with $\theta_0 = -\arcsin\left(-\frac{\sqrt{3\,X^2-2}}{X^2}\right)$.
  But we have $h_{\theta=\frac{\pi}{2}}(X) > 0$ and $h_{\theta=0}(X) = \Phi_1(X) + X\,g_1(X) < 0$ (using Proposition 4).
  Therefore, we have a zero when $-1 < X \leq -\sqrt{\frac{2}{3}}$.

Therefore, we find one zero of h (and only one) when $X > 1$ or when $-1 < X < \gamma_0$.

□

Corollary 1 *$\nabla^2 F(x,0)$ has two extrema values in x_0 and x_1 with $-\sigma < x_0 < \gamma_0\,\sigma < 0$ and $\frac{\sigma}{\sin\theta} < x_1 < \frac{\sqrt{3}\sigma}{\sin\theta}$. The first one $(x_0, 0)$ corresponds to a hyperbolic point of $\nabla^2 F(x,y)$, the second one $(x_1, 0)$ corresponds to an extremum point of $\nabla^2 F(x,y)$. We also have $\nabla^2 F(x_0,0) = \Theta\left(\frac{(A_1-A_0)\sin\theta}{\sigma^2}\right)$ and $\nabla^2 F(x_1,0) = \Theta\left(\frac{A_1-A_0}{\sigma^2}\right)$.*

Moreover when θ goes through $]0, \frac{\pi}{2}[$, x_0 (respectively x_1) take all values in $]-\sigma, \gamma_0\,\sigma[$ (respectively in $]\sigma, \infty[$).

Proof :

From Theorems 1 and 2 and using the fact that $G(X,Y)$ is symmetric in Y, we get :

- $G(X,0)$ has two extrema values in X_0 and X_1,
- $(X_0, 0)$ is a hyperbolic point of $G(X,Y)$,
- $(X_1, 0)$ is an extremum point of $G(X,Y)$.

The first part of the corollary follows from Proposition 3, $\sqrt{3-\sqrt{9-8\,\sin^2\theta}} < \sqrt{2}\sin\theta$ and $\sqrt{3+\sqrt{9-8\,\sin^2\theta}} < \sqrt{6}$ and Theorem 3 (for $X_0 < \gamma_0\sigma$).
Using Proposition 3, we obtain :

$$\nabla^2 F(x_0,0) = \frac{A_1-A_0}{\sigma^2} G(X_0,0) = 2\frac{A_1-A_0}{\sigma_2}\left(-X_0\,\sin\theta\, g_1(X_0\,\sin\theta)\,\Phi_1(X_0\,\cos\theta)\right).$$

Using $-1 \leq X_0 \leq \gamma_0$: $g_1(X_0\,\sin\theta) = \Theta(1)$, $\Phi_1(X_0\,\cos\theta) = \Theta(1)$ and $\nabla^2 F(x_0,0) = \Theta\left(\frac{(A_1-A_0)\sin\theta}{\sigma^2}\right)$.
Similarly, we get :

$$\nabla^2 F(x_1,0) = \frac{A_1-A_0}{\sigma^2} G(X_1,0) = 2\frac{A_1-A_0}{\sigma_2}\left(-X_1\,\sin\theta\, g_1(X_1\,\sin\theta)\,\Phi_1(X_1\,\cos\theta)\right),$$

with $X_1\,\sin\theta = \Theta(1)$, $g_1(X_1\,\sin\theta) = \Theta(1)$ and $\frac{1}{2} \leq \Phi_1(X_1\,\cos\theta) = \Theta(1) \leq 1$ and so $\nabla^2 F(x_1,0) = \Theta\left(\frac{A_1-A_0}{\sigma^2}\right)$.
The last part of the corollary follows from Theorem 3.

□

Study of the extrema of $\nabla^2 F$

Let note $U = U_0 = Y\cos\theta + X\sin\theta$,$V = V_0 = X\cos\theta - Y\sin\theta$, $\theta_2 = 2\theta$, then we have $X = U\sin\theta + V\cos\theta, Y = U\cos\theta - V\sin\theta$, $U_1 = U\cos\theta_2 - V\sin\theta_2$ and $V_1 = U\sin\theta_2 + V\cos\theta_2$.

Therefore $G(X,Y) = H(U,V)$ with

$$\begin{aligned} H(U,V) &= (U\cos\theta_2 - V\sin\theta_2)g_1(U\cos\theta_2 - V\sin\theta_2)\Phi_1(U\sin\theta_2 + V\cos\theta_2) \\ &\quad -U\,g_1(U)\Phi_1(V). \end{aligned}$$

Let note :

- $K(X) = \epsilon\sqrt{1+X\,J(X)}$ with $\epsilon \in \{-1,1\}$,
- and $l(X) = \Phi_1(\sin\theta_2\,K(X) + \cos\theta_2\,X) + \frac{(\sin\theta_2\,K(X)+\cos\theta_2\,X)\,g_1(\sin\theta_2\,K(X)+\cos\theta_2\,X)}{1-(\cos\theta_2\,K(X)-\sin\theta_2\,X)^2}$.

First, we give some basic properties about $J(X)$ and $X^2 + K(X)^2$ which will be used on the following :

Proposition 5 *We have :*

1. *when* $X \geq 0$, $0 < J(X) \leq \frac{2}{\sqrt{2\,\pi}} < 1$,
2. *when* $\gamma_0 \leq X \leq 0$, $0 < \frac{2}{\sqrt{2\,\pi}} \leq J(X) < \sqrt{2}$,
3. *when* $X \geq \gamma_0$, $J(X) + 1.5\,X > 0$,
4. *when* $X > -1$, $0 < (1+X)\,J(X) < 1$.
5. *when* $X \geq \gamma_0$, $(X + J(X))(1 - X\,J(X)) + X > 0$.

Proof :

- Indeed, we have $J'(X) = -\frac{g_1(X)}{\Phi_1^2(X)}\,(X\Phi_1(X) + g(X))$. But we can show easily that $X\Phi_1(X) + g(X)$ is increasing and that $\gamma_0\Phi_1(\gamma_0) + g(\gamma_0) = g(\gamma_0)(1 - \gamma_0^2) > 0$ (by definition of γ_0). Therefore $J'(X) < 0$ when $X > \gamma_0$ and $J(X)$ is decreasing. Using $J(0) = \frac{\frac{1}{\sqrt{2\pi}}}{\frac{1}{2}}$ and $J(X) > 0$, we obtain the first part of the proposition.

  Using $J(\gamma_0) = -\frac{1}{\gamma_0}$ (by definition of γ_0) and $\gamma_0 < -\frac{\sqrt{2}}{2}$ (see Proposition 4), we get the second part of the proposition.
- Indeed, this is equivalent to prove that $m(X) = g_1(X) + 1.5\,X\,\Phi_1(X) > 0$ when $X \geq \gamma_0$. But we have $m'(X) = \frac{X\,g_1(X) + 3\,\Phi_1(X)}{2}$, which is clearly positive when $X \geq 0$.

  When $\gamma_0 \leq X < 0$, we have $m''(X) = \frac{(4 - X^2)\,g_1(X)}{2} > 0$. So $m'(X)$ is increasing and we have also $m'(X) > m'(\gamma_0) = \Phi_1(\gamma_0) > 0$.

  Therefore when $X \geq \gamma_0$, m is increasing. But using Proposition 4, $m(\gamma_0) = g_1(\gamma_0)(1 - 1.5\gamma_0^2) > 0$. This ends this part of the proof.
- The first part, $0 < (1 + X)\,J(X)$ is clearly true. The second part is equivalent to prove that $m(X) = (1 + X)g_1(X) - \Phi_1(X) < 0$.

  But we have $m'(X) = -X(1 + X)g_1(X)$. So $m(X)$ is increasing when $X \in [-1, 0]$ and is decreasing when $X \geq 0$. But $m(0) = \frac{1}{\sqrt{2\pi}} - \frac{1}{2} < 0$. This ends the proof.
- When $\gamma_0 \leq X < 0$, The point 5.4 gives $1 - X\,J(X) > J(X)$. From 5.3 we know that $J(X) + 1.5\,X > 0$ and therefore $J(X) + X > 0$. Furthermore we know that $J(X) > \frac{2}{\sqrt{2\,\pi}}$ and $(X + J(X))(1 - X\,J(X)) + X > J(X)(X + J(X)) + X > \frac{X}{2} + \frac{2}{\pi}$ which is greater than zero when $\gamma_0 < X < 0$.

  When $X \geq 0$, the previous point gives $1 - X\,J(X) > J(X)$. Therefore $(X + J(X))(1 - X\,J(X)) + X > J(X)(X + J(X)) + X > 0$.

□

Proposition 6 *In the interval* $[\gamma_0, \infty[$, $X^2 + K^2(X)$ *is continue and strictly increasing from* γ_0^2 *to* ∞.

Proof :

Let $m(X) = X^2 + K^2(X)$.

We have $m(X) = X^2 + 1 + \frac{X\,g_1(X)}{\Phi_1(X)}$, therefore :

$$\begin{aligned} m'(X) &= 2\,X + \frac{g_1(X)}{\Phi_1(X)^2}\left((1 - X^2)\Phi_1(X) - X\,g_1(X)\right) \\ &= 2\,X + (1 - X^2)J(X) - X\,J^2(X) \end{aligned}$$

with $J(X) = \frac{g_1(X)}{\Phi(X)}$.

- when $\gamma_0 \leq X < 0$,

  Indeed, let $h(Y) = -\frac{1}{2} + X\,Y + Y^2$. The roots of $h(Y) = 0$ correspond to $\frac{-X - \sqrt{X^2+2}}{2}$ and $\frac{-X + \sqrt{X^2+2}}{2}$. Using Proposition 4 we have :

$$\frac{-X + \sqrt{X^2 + 2}}{2} < \frac{-X + \sqrt{X^2 + \frac{8}{\pi}}}{2} \leq J(X).$$

Therefore $h(J(X)) > 0$ and $m'(X) = -X\,(h(J(X)) - 1.5) + J(X) \geq 1.5\,X + J(X)$.
Using Proposition 5, we get $m'(X) > 0$.

- when $0 \geq X \geq 1$,
  we have $1 - X^2 \geq 0$ and $2 - J^2(X) > 0$ (using Proposition 5), so $m'(X) > 0$.
- when $1 < X$,
  using Proposition 5, we have $(1 + X)J(X) < 1$ and $J(X) < 1$. So $(1 - X^2)J(X) > -(X - 1)$ and $m'(X) > 2\,X - X + 1 - X = 1$,

So m is an increasing function in X and is continue in X. We can note that $m(\gamma_0) = \gamma_0^2$, $\lim_{X\to\infty} m(X) = \infty$. This ends the proof of the proposition.

□

Then, we have the following theorem :

Theorem 4 *The extrema and the hyperbolic points of H (and so of $\nabla^2 F$) are the points $(K(V), V)$ such that $l(V) = 0$.*

Proof :

Indeed, a point (U, V) is an extremum or a hyperbolic point of H if and only if $\frac{\delta H(X,Y)}{\delta X}(U, V) = 0$ and $\frac{\delta H(X,Y)}{\delta Y}(U, V) = 0$.
However we have :

$$\frac{\delta H(U,V)}{\delta U} = \cos\theta_2\, g_1(U\cos\theta_2 - V\sin\theta_2)\,\Phi_1(U\sin\theta_2 + V\cos\theta_2)\left(1 - (U\cos\theta_2 - V\sin\theta_2)^2\right)$$
$$+ g_1(U)\left(\sin\theta_2(U\cos\theta_2 - V\sin\theta_2)g_1(V) - \Phi_1(V)(1 - U^2)\right). \qquad (7)$$

and

$$\frac{\delta H(U,V)}{\delta V} = -\sin\theta_2 g_1(U\cos\theta_2 - V\sin\theta_2)\Phi_1(U\sin\theta_2 + V\cos\theta_2)\left(1 - (U\cos\theta_2 - V\sin\theta_2)^2\right)$$
$$+ g_1(U)g_1(V)\left(\cos\theta_2(U\cos\theta_2 - V\sin\theta_2) - U\right). \qquad (8)$$

Therefore, if we combine Equations (7) and (8), using the following combination $\sin\theta_2$(Equation(7))$+\cos\theta_2$(Equation(8)) and $\cos\theta_2$(Equation(7))$-\sin\theta_2$(Equation(8)), we obtain :

$$0 = -\sin\theta_2\, g(U)\,\left(V\, g_1(V) + (1 - U^2)\Phi_1(V)\right),$$

and

$$\begin{aligned} 0 &= \left(1 - (\cos\theta_2\, U - \sin\theta_2\, V)^2\right) g_1(\cos\theta_2\, U - \sin\theta_2\, V)\Phi_1(\sin\theta_2\, U + \cos\theta_2\, V) \\ &\quad + g_1(U)\left(-\cos\theta_2(1 - U^2)\Phi_1(V) + \sin\theta_2\, U\, g_1(V)\right) \\ &= g_1(\cos\theta_2\, U - \sin\theta_2\, V) \\ &\quad \left(\left(1 - (\cos\theta_2\, U - \sin\theta_2\, V)^2\right)\Phi_1(\sin\theta_2\, U + \cos\theta_2\, V) + \right. \\ &\quad \left.(\sin\theta_2\, U + \cos\theta_2\, V)g_1(\sin\theta_2\, U + \cos\theta_2\, V)\right) \end{aligned}$$

The first equation is equivalent to $U = K(V)$ and the second equation is equivalent to $l(V) = 0$ if and only if there is no solution which verify $(\cos\theta_2\, U -$

$\sin\theta_2\, V)^2 = 1$ and $\sin\theta_2\, U + \cos\theta_2\, V = 0$ (with $U = K(V)$). We will show this in the following.

Indeed these equations are equivalent to $U = \epsilon' \cos\theta_2$, $V = -\epsilon' \sin\theta_2$ (with $U = K(V)$ and $\epsilon' \in \{-1, 1\}$). Therefore, we must prove that

$$cos^2\theta_2 = 1 + \frac{\epsilon' \sin\theta_2 g_1(\epsilon' \sin\theta_2)}{\Phi_1(\epsilon' \sin\theta_2)}$$

has no solution.

This is clearly true when $\epsilon' = 1$. When $\epsilon' = -1$, this equation is equivalent to prove that :

$$-\sin\theta_2 \Phi_1(-\sin\theta_2) + g_1(-\sin\theta_2) = 0$$

has no solution.

Let $m(X) = \Phi_1(X) + \frac{g_1(X)}{X}$, we have $m'(X) = -\frac{g_1(X)}{X^2}$, $\lim_{-\infty} m = 0$, $lim_{X\to 0-} m(X) = -\infty$, $\lim_{X\to 0+} m(X) = +\infty$, $\lim_{+\infty} m = 1$. Therefore $m(X)$ is a decreasing function and there exists no solution to $m(X) = 0$. This ends the proof.

□

Corollary 2 *(U, V) is a extremum or a hyperbolic point of H implies that V must be greater or equal to γ_0.*

Proof :

Using the previous theorem, we must have $U = K(V)$ but this implies that $1 + \frac{V\, g_1(V)}{\Phi_1(V)} \geq 0$. Proposition 4 ends the proof.

□

Theorem 5

- *When $\epsilon = 1$, for each $X > 0$ there exists one and only one $\theta \in]0, \frac{\pi}{2}[$, such that $l(X) = 0$ and none when $\gamma_0 \leq X \leq 0$,*
- *When $\epsilon = -1$, for each $\gamma_0 < X < 0$ there exists one and only one $\theta \in]0, \frac{\pi}{2}[$, such that $l(X) = 0$ and none when $X \geq 0$.*

Proof :

Indeed, if we set the value of X and note :

- $u(\theta') = \cos\theta' K(X) - \sin\theta' X$,
- $v(\theta') = \sin\theta' K(X) + \cos\theta' X$,
- $m(\theta') = \Phi_1(v(\theta')) + \frac{v(\theta')\, g_1(v(\theta'))}{1-u(\theta')^2}$,
- $M(\theta') = 2 - (X^2 + K(X)^2)(3 - u(\theta')^2)$.

We can note that $m(\theta') = l(X)$ when $\theta' = \theta_2$. So in order to find the value θ in $]0, \frac{\pi}{2}[$ such that $l(X) = 0$, we will study the variations of the function $m(\theta')$ when θ' goes through $]0, \pi[$.

We have $u'(\theta') = -v(\theta')$ and $v'(\theta') = u(\theta')$, so

$$\begin{aligned} m'(\theta') &= \frac{u(\theta')\, g_1(v(\theta'))}{(1-u(\theta')^2)^2}(2 - (X^2 + K(X)^2)(3 - u(\theta')^2)) \\ &= \frac{u(\theta')\, g_1(v(\theta'))}{(1-u(\theta')^2)^2} M(\theta') \end{aligned}$$

and $M'(\theta') = -2u(\theta')v(\theta')(X^2 + K(X)^2)$.
Therefore we will need to study the signs of $m'(\theta')$ and $M'(\theta')$ and so the signs of $u(\theta')$, $v(\theta')$, $M(\theta')$.
Before beginning these studies, let introduce some notations :

- for simplicity, we will denote by $atan(x, y)$ the function which gives the arctan value of $\frac{x}{y}$ which corresponds to an angle in $[0, \pi]$ (with $atan(0, y) = 0$ if $y > 0$ and $atan(0, y) = \pi$ if $y < 0$),
- $\alpha_0 = atan(K(X), X)$ is the only value θ in $[0, \pi]$ such that $u(\theta') = 0$ (the limits of the interval 0 or π are only reached when $X = \gamma_0$),
- $\alpha_1 = atan(X, -K(X))$ is the only value θ in $[0, \pi]$ such that $v(\theta') = 0$ (the limits of the interval 0 or π are only reached when $X = 0$),

Lemma 2 *Let us note :*

- ζ_0 *is the only value such that* $X^2 + K(X)^2 = \frac{2}{3}$,
- ζ_1 *is the only value such that* $X^2 + K(X)^2 = 2$,

then

- $m(0) = 0$ *when* $X \neq 0$,
- $m(\pi) = 1$ *when* $X \neq 0$,
- *when* $\epsilon = 1$, $m(\alpha_0) > 0$ *when* $X \neq \gamma_0$,
- *when* $\epsilon = -1$, $m(\alpha_0) < 0$ *when* $X \neq \gamma_0$,
- $M(0) = M(\pi) = 0$ *if and only if* $X = 0$ *and* $M(0) = M(\pi) > 0$ *if and only* $\gamma_0 \leq X < 0$.
- $M(\alpha_0) = 0$ *if and only if* $X = \zeta_0$ *and* $M(\alpha_0) > 0$ *if and only if* $\gamma_0 \leq X < \zeta_0$,
- $M(\alpha_1) = 0$ *if and only if* $X = 0$ *or* $X = \zeta_1$ *and* $M(\alpha_1) < 0$ *if and only if* $0 < X < \zeta_1$.

Proof :

Proposition 6 proves the existence of ζ_0 and ζ_1 and gives us $\gamma_0 < \zeta_0 < 0 < \zeta_1$.

- We have $u(0) = K(X)$, $v(0) = X$, therefore $m(0) = \Phi_1(X) + \frac{X\, g_1(X)}{1 - K^2(X)} = \Phi_1(X) - \Phi_1(X) = 0$,
- We have $u(\pi) = -K(X)$, $v(\pi) = -X$, therefore $m(\pi) = \Phi_1(-X) + \frac{-X\, g_1(-X)}{1 - K^2(X)} = \Phi_1(-X) + \Phi_1(X) = \Phi_1(-X) + (1 - \Phi_1(-X)) = 1$,
- We have $u(\alpha_0) = 0, \cos\alpha_0 = \epsilon\frac{X}{\sqrt{X^2 + K(X^2)}}$, $\sin\alpha_0 = \epsilon\frac{K}{\sqrt{X^2 + K(X^2)}}$. Therefore, $v(\alpha_0) = \epsilon\sqrt{X^2 + K(X^2)}$ and $m(\alpha_0) = \Phi_1(v(\alpha_0)) + v(\alpha_0)g(v(\alpha_0))$. When $\epsilon = 1$, $m(\alpha_0)$ is clearly positive. When $\epsilon = -1$, using Proposition 6 $v(\alpha_0) < \gamma_0$ and using Proposition 3 $m(\alpha_0) < 0$.

- We have

$$\begin{aligned} M(0) = M(\pi) &= 2 - (X^2 + K(X)^2)(3 - K(X)^2) \\ &= -X\left((X + J(X))(1 - X\,J(X)) + X\right) \end{aligned}$$

  Proposition 5 gives the sign of $M(0)$ and $M(\pi)$,
- indeed, we have by definition $u(\alpha_0) = 0$ and therefore $M(\alpha_0) = 2 - 3(X^2 + K(X)^2)$. Then, $M(\alpha_0)$ has only one zero when $X = \zeta_0$ and $M(\alpha_0) < 0$ when $X > \zeta_0$.
- This time, we have $u^2(\alpha_1) + v^2(\alpha_1) = X^2 + K^2(X)$ therefore $M(\alpha_1) = (2 - X^2 - K(X)^2)(1 - X^2 - K(X)^2)$ and $M(\alpha_1) = 0$ when $X = 0$ or $X = \zeta_1$ and $M(\alpha_1) < 0$ when $0 < X < \zeta_1$.

□

To prove the theorem 5, we will split the demonstration into many parts, differencing the cases ϵ equals 1 or -1; the cases X negative and positive; the case $X = 0$ and $X = \gamma_0$.

- When $X = 0$:

  In this case, $u(\theta') = \epsilon \cos\theta'$, $v(\theta') = \epsilon \sin\theta'$, $m(\theta') = f(v(\theta'))$ with $f(x) = \Phi_1(x) + \frac{g_1(x)}{x}$. But f is decreasing (by derivation) between $[-1, 0[$ from $f(-1)$ down to $-\infty$ and between $]0, 1]$ from ∞ down to $f(1)$. $f(1)$ is clearly positif. Using Proposition 4, we obtain $1 < \frac{1+\sqrt{1+\frac{8}{\pi}}}{2} \leq \frac{g_1(-1)}{\Phi_1(-1)}$ and $f(-1) < 0$. Therefore $f(x) = 0$ has no solution when $x \in [-1, 1]$ and $m(\theta') = 0$ has no solution when $\theta' \in]0, \pi[$.
- When $X = \gamma_0$:

  We have $u(\theta') = -\gamma_0 \sin\theta' > 0$ and $v(\theta') = \gamma_0 \cos\theta'$. Therefore $M'(\theta') > 0$ when $\theta' \in]0, \frac{\pi}{2}[$ and $M'(\theta') < 0$ when $\theta' \in]\frac{\pi}{2}\pi[$. As $M(0) > 0$ and $M(\pi) > 0$, we have in this case $M(\theta') > 0$ when $\theta' \in [0, \pi]$. Therefore $m'(\theta') > 0$ when $\theta' \in]0, \pi[$ and $m(\theta')$ is increasing in $[0, \pi]$ from 0 up to 1. Then $m(\theta') = 0$ has no solution when $\theta' \in]0, \pi[$.
- When $\epsilon = 1$ and $X > 0$:

  In this case, we clearly obtain :

  - $0 < \alpha_0 < \frac{\pi}{2} < \alpha_1 < \pi$,
  - $u(\theta') > 0$ if and only if $0 \leq \theta' < \alpha_0$,
  - $v(\theta') > 0$ if and only if $0 \leq \theta' < \alpha_1$,
  - $K(X) > 1$.

  Therefore $u(\theta')$ decreases from $K(X)$ to $-\sqrt{K(X)^2 + X^2}$ when $\theta' \in [0, \alpha_1]$ and increases to $-K(X)$ when $\theta' \in [\alpha_1, \pi]$. As $K(X) > 1$ when $X > 0$, $u(\theta')^2 = 1$ has two solutions β_0 and β_1 with $0 \leq \beta_0 < \alpha_0 < \beta_1 \leq \alpha_1$.

  Since $M'(\theta')$ has the same sign than $-u(\theta')\,v(\theta')$, M decreases in $[0, \alpha_0]$ from $M(0) < 0$ down to $M(\alpha_0) < 0$, increases in $[\alpha_0, \alpha_1]$ up to $M(\alpha_1)$ and decreases in $[\alpha_1, \pi]$ to $M(\pi) < 0$.

  Therefore two cases arise :

- When $X \leq \zeta_1$, $M(\alpha_1) \leq 0$. Therefore $m'(\theta') < 0$ if $0 < \theta' < \alpha_0$ and $m'(\theta') > 0$ if $\alpha_0 < \theta'$ (excepted in α_1 if $X = \zeta_1$). m is decreasing in $[0, \beta_0[$ from $m(0) = 0$ down to $-\infty$, is decreasing in $]\beta_0, \alpha_0]$ from ∞ down to $m(\alpha_0) > 0$, is increasing in $[\alpha_0, \beta_1[$ from to $m(\alpha_0) > 0$ to ∞ and is increasing in $]\beta_1, \pi]$ from $-\infty$ to $m(\pi) = 1$. $m(\theta') = 0$ has always one (and only one) solution when $\theta' \in]0, \pi[$.
- When $X > \zeta_1$, $M(\theta') < 0$ when $0 < \theta' < \rho_0$ and when $\pi > \theta' > \rho_1$ with ρ_0 and ρ_1 the values which correspond to the values of $M(\theta') = 0$ (and with $\alpha_0 \leq \beta_1 < \rho_0 < \alpha_1 < \rho_1$ because $M(\beta_1) = 2(1 - X^2 - K^2(X)) < 0$) and $M(\theta') > 0$ when $\rho_0 < \theta' < \rho_1$. Therefore the variations of $m(\theta')$ differ only from the previous case when $\beta_1 \geq \theta'$. Then, $m(\theta')$ is increasing in $]\beta_1, \rho_0]$ from $-\infty$ to $m(\rho_0)$, then is decreasing in $[\rho_0, \rho_1]$ from $m(\rho_0)$ down to $m(\rho_1) > 0$ (indeed as $\beta_1 < \alpha_1 < \rho_1$, we have $v(\rho_1) < 0$ and $1 - u^2(\rho^1) < 1 - 1 = 0$) and finally is increasing in $[\rho_1, \pi]$ from $m(\rho_1)$ to $m(\pi) = 1$. Therefore as in the previous case, $m(\theta') = 0$ has always one (and only one) solution when $\theta' \in]0, \pi[$.

- When $\epsilon = 1, \gamma_0 < X < 0$

  In this case, we clearly obtain :

  - $0 < \alpha_1 < \frac{\pi}{2} < \alpha_0 < \pi$,
  - $u(\theta') > 0$ if and only if $0 \leq \theta' < \alpha_0$,
  - $v(\theta') > 0$ if and only if $\alpha_1 < \theta'$,
  - $0 < K(X) < 1$.

  Therefore u increases from $K(x)$ to $\sqrt{K(X)^2 + X^2}$ when $\theta' \in [0, \alpha_1]$ and decreases to $-K(X)$ when $\theta' \in [\alpha_1, \pi]$. Because $K^2(X) + X^2 < 1$(using Proposition 6) and $K(X) < 1$, $u^2(\theta') = 1$ has no solution in this interval.

  As $M'(\theta')$ has the same sign than $-u(\theta')\, v(\theta')$, M increases in $[0, \alpha_1]$ from $M(0) = 0$ up to $M(\alpha_1) > 0$, decreases in $[\alpha_1, \alpha_0]$ down to $M(\alpha_0)$ and increases in $[\alpha_0, \pi]$ up to $M(\pi) > 0$.

  Two cases appear :

  - When $X \leq \zeta_0$, $M(\alpha_0) \geq 0$. Therefore $M(\theta') > 0$ (excepted when $\theta' = \alpha_0$ and $X = \zeta_0$ where it is equal to 0). So $m(\theta')$ is increasing in $[0, \alpha_0]$ from $m(0) = 0$ up to $m(\alpha_0) > 0$ and is decreasing in $[\alpha_0, \pi]$ down to $m(\pi) = 1$. So $m(\theta') = 0$ has no solution when $\theta' \in]0, \pi[$.
  - When $X > \zeta_0$, $M(\alpha_0) < 0$. Therefore $M(\theta') > 0$ when $0 < \theta' < \rho_0$ and when $\pi > \theta' > \rho_1$ with ρ_0 and ρ_1 the values which correspond to the values of $M(\theta') = 0$ (and with $\alpha_1 < \rho_0 < \alpha_0 < \rho_1$) and $M(\theta') < 0$ when $\rho_0 < \theta' < \rho_1$. So $m(\theta')$ is increasing in $[0, \rho_0]$ from $m(0) = 0$ up to $m(\rho_0)$, is decreasing in $[\rho_0, \alpha_0]$ down to $m(\alpha_0) > 0$, is increasing in $[\alpha_0, \rho_1]$ up to $m(\rho_1)$ and is decreasing in $[\rho_1, \pi]$ down to $m(\pi) = 1$. So $m(\theta') = 0$ has no solution when $\theta' \in]0, \pi[$.

- $\epsilon = -1$ and $X > 0$. In this case we clearly obtain :
  - $0 < \alpha_1 < \frac{\pi}{2} < \alpha_0 < \pi$,
  - $u(\theta') > 0$ if and only if $\theta' > \alpha_0$,
  - $v(\theta') > 0$ if and only if $0 < \theta' < \alpha_1$,
  - $K(X) < -1$.

Therefore u decreases from $K(x)$ to $-\sqrt{K(X)^2+X^2}$ when $\theta' \in [0,\alpha_1]$ and increases to $-K(X)$ when $\theta' \in [\alpha_1,\pi]$. Since $K(X) < -1$ when $X > 0$, $u^2(\theta') = 1$ has two solutions β_0 and β_1 such that $\alpha_1 < \beta_0 < \alpha_0 < \beta_1$.

As $M'(\theta')$ has the same sign than $-u(\theta')\,v(\theta')$, M increases in $[0,\alpha_1]$ from $M(0) < 0$ to $M(\alpha_1)$, decreases in $[\alpha_1,\alpha_0]$ to $M(\alpha_0) < 0$ and increases in $[\alpha_0,\pi]$ to $M(\pi) < 0$.

Two cases appear :

- When $0 < X \leq \zeta_1$, $M(\alpha_1) \leq 0$. Therefore $m'(\theta') > 0$ if $0 < \theta' < \alpha_0$ and $m'(\theta') < 0$ if $\alpha_0 < \theta'$ (excepted in α_1 if $X = \zeta_1$). m is increasing in $[0,\beta_0[$ from $m(0) = 0$ to ∞, increasing in $]\beta_0,\alpha_0]$ from $-\infty$ to $m(\alpha_0) < 0$, decreasing in $[\alpha_0,\beta_1[$ to $-\infty$ and decreasing in $]\beta_1,\pi]$ from ∞ down to $m(\pi) = 1$. Therefore, $m(\theta') = 0$ has no solution when $]0,\pi[$.
- When $X > \zeta_1$, $M(\alpha_1) > 0$. Therefore $M(\theta') < 0$ for $\theta' \in [0,\rho_0]$ and $\theta' \in [\rho_1,\pi]$ where ρ_0 and ρ_1 the values which verify $M(\theta') = 0$ (and with $0 < \rho_0 < \alpha_1 < \rho_1 < \beta_0 < \alpha_0$ because $M(\beta_0) = 2(1 - X^2 - K^2(X)) > 0$). m' is positive in $[0,\rho_0]$ and $[\rho_1,\alpha_0]$ and negative in $[\rho_0,\rho_1]$ and $[\alpha_0,\pi]$. Therefore the variations of $m(\theta')$ differ only from the previous case when $\theta' \leq \beta_0$. Then, m is increasing in $[0,\rho_0]$ from $m(0) = 0$ to $m(\rho_0)$, decreasing in $[\rho_0,\rho_1[$ down to $m(\rho_1) > 0$ (because $\alpha_1 < \rho_1 < \beta_0$, we $v(\rho_1) < 0$ and $1 - u^2(\rho_1) < 0$) and increasing in $[\rho_1,\beta_0[$ from $m(\rho_1)$ to ∞. Therefore, as in the previous case, $m(\theta') = 0$ has no solution when $]0,\pi[$.

- $\epsilon = -1$ and $\gamma_0 < x < 0$, In this case we clearly obtain :
  - $0 < \alpha_0 < \frac{\pi}{2} < \alpha_1 < \pi$,
  - $u(\theta') > 0$ if and only if $\theta' > \alpha_0$,
  - $v(\theta') > 0$ if and only if $\theta' > \alpha_1$,
  - $-1 < K(X) < 0$.

  Therefore u increases from $K(x)$ to $\sqrt{K(X)^2+X^2}$ when $\theta' \in [0,\alpha_1]$ and decreases down to $-K(X)$ when $\theta' \in [\alpha_1,\pi]$. Since $K^2(X) + X^2 < 1$(using Proposition 6) and $-1 < K(X)$, $u^2(\theta') = 1$ has no solution in this interval.

  As $M'(\theta')$ has the same sign than $-u(\theta')\,v(\theta')$, M decreases in $[0,\alpha_0]$ from $M(0) > 0$ to $M(\alpha_0)$, increases in $[\alpha_0,\alpha_1]$ to $M(\alpha_1) > 0$ and decreases in $[\alpha_1,\pi]$ to $M(\pi) > 0$.

  Two case appear :

  - When $\gamma_0 < X \leq \zeta_0$, $M(\alpha_0) \geq 0$. Therefore $M(\theta') > 0$ for $\theta' \in [0,\pi]$ and $m'(\theta') < 0$ for $\theta' \in [0,\alpha_0[$ and $m'(\theta') > 0$ for $\theta' \in]\alpha_0,\pi]$. Therefore m is decreasing in $[0,\alpha_0]$ from $m(0) = 0$ down to $m(\alpha_0) < 0$ and increasing in $[\alpha_0,\pi]$ to $m(\pi) = 1$. $m(\theta') = 0$ has always one and only one solution when $\theta' \in]0,\pi[$.
  - When $\zeta_0 < X < 0$, $M(\alpha_0) < 0$. Therefore $M(\theta') > 0$ for $\theta' \in [0,\rho_0]$ and $\theta' \in [\rho_1,\pi]$ where ρ_0 and ρ_1 the values which verify $M(\theta') = 0$ ($0 < \rho_0 < \alpha_0 < \rho_1 < \alpha_1$). Thus, $m(\theta')$ is decreasing in $[0,\rho_0]$ from 0 down to $m(\rho_0)$, increasing in $[\rho_0,\alpha_0]$ to $m(\alpha_0) < 0$, decreasing in

$[\alpha_0, \rho_1]$ to $m(\rho_1)$ and increasing in $[\rho_1, \pi]$ to $m(\pi) = 1$. Therefore $m(\theta') = 0$ has always one and only one solution when $\theta' \in]0, \pi[$.

□

Theorem 6 *If (X, Y) is an extremum or an hyperbolic point of $G(X, Y)$ then $Y = 0$.*

Proof :

Indeed using Theorem 4, we must have $l(V) = 0$ with $V = X\cos\theta - Y\sin\theta$ and $U = Y\cos\theta + X\sin\theta = K(V)$.

Using Theorem 3, we know that when θ varies in $]0, \frac{\pi}{2}[$, there is one and only one extremum or hyperbolic point of $G(X, 0)$ when $-1 < X < \gamma_0$ and $1 < X$.

As $K(V) = U$ and $U^2 + V^2 = X^2 + Y^2$, we must have on theses points $K^2(V) + V^2 = X^2$. Using Proposition 6, $K^2(V) + V^2$ is continue, and strictly increasing from γ_0^2 to ∞. This means that each of these values X (which verify $-1 < X < \gamma_0$ or $1 < X$) corresponds to one and one only value V which verifies $K^2(V) + V^2 = X^2$ for each $\gamma_0 < V < 0$ or for each $0 < V$.

Using $l(V) = 0$ and Theorem 5, this property shows that the extremum and the hyperbolic points of $G(X, 0)$ when θ goes through $]0, \frac{\pi}{2}[$ are the same than the extremum and hyperbolic points of $G(X, Y)$ when θ goes through $]0, \frac{\pi}{2}[$.

□

With Proposition 3, we obtain easily the following corollary :

Corollary 3 *The extremum and the hyperbolic points of $\nabla^2 F$ are on the straight line $y = 0$.*

Bibliography

[1] S. Ando. "Image Field Categorization and Edge/Corner Detection from Gradient Covariance", *IEEE Transactions on PAMI*, vol. 22, no. 2, pp. 179–190, Feb. 2000.

[2] H. Asada and M. Brady. "The Curvature Primal Sketch", *IEEE Transactions on PAMI*, vol. 8, no. 1, pp. 2–14, Jan. 1986.

[3] V. Berzins. "Accuracy of Laplacian Edge Detectors", *Computer Vision, Graphics and Image Processing*, vol. 27, no. 1, pp. 195–210, July, 1984.

[4] J. Cooper, S. Venkatesh and L. Kitchen. "Early Jump-Out Corner Detectors", *IEEE Transactions on PAMI*, vol. 15, no. 8, pp. 823–828, Aug. 1993.

[5] E. de Micheli, B. Caprile, P. Ottonello, and V. Torre. "Localization and Noise in Edge Detection", *IEEE Transactions on PAMI*, vol. 11, no. 10, pp. 1106–1116, Oct. 1989.

[6] R. Deriche and T. Blaszka. "Recovering and Characterizing Image Features Using An Efficient Model Based Approach", In *Proceedings of IEEE Conference on Computer Vision and Pattern Recognition*, pp. 530–535, June 1993, New York, USA.

[7] R. Deriche and G. Giraudon. "A Computational Approach for Corner and Vertex Detection", *International Journal of Computer Vision*, vol. 10, no. 2, pp. 101–124, Feb. 1993.

[8] R. Espelid and I. Jonassen. "A Comparison of Splitting Methods for the Identification of Corner Points", *Pattern Recognition Letters*, vol. 12, no. 2, pp. 79–83, Feb. 1991.

[9] W. F*ö*rtsner and E. G*ü*lch. "A Fast Operator for Detection and Precise Location of Distinct Points, Corners and Centres of Circular Features", In *Proceedings of the Intercommission Conference on Fast Processing of Photogrammetric Data*, Switzerland, June 1987.

[10] S. Ghosal and R. Mehrotra. "A Moment Based Unified Approach to Image Feature Detection", In *IEEE Trans. Image Processing*, vol. 6, no. 6, pp. 781–793, June 1997.

[11] A. Guiduci. “Corner Characterization by Differential Geometry Techniques”, Pattern Recognition Letters, vol. 8, no. 5, pp. 311–318, Dec. 1988.

[12] B. Luo, A.D.J.Cross and E.R. Hancock. “Corner Detection via Topographic Analysis of Vector Potential”, *Pattern Recognition Letters*, vol. 20, no. 6, pp. 635–650, June 1999.

[13] F. Mokhtarian and R. Suomela. “Robust Image Corner Detection Through Curvature Scale Space”, *IEEE Transactions on PAMI*, vol 20, no. 12, pp. 1376–1381, Dec. 1998.

[14] J. A. Noble. “Finding Corners”, *Image and Vision Computing*, vol. 6, no. 2, pp. 121–128, May 1988.

[15] A. Rattarangsi and R. T. Chin. “Scale-Based Detection of Corners of Planar Curves”, *IEEE Transactions on PAMI*, vol. 14, no. 4, pp. 430–449, April 1992.

[16] K. Rohr. “Recognizing Corners by Fitting Parametric Models”, *International Journal of Computer Vision*, vol. 9, no. 3, pp. 213–230, Dec. 1992.

[17] K. Rohr. “Localization properties of direct corner detectors”, *Journal of Mathematical Image and Vision*, vol. 4, no. 2, pp. 139–150, 1994.

[18] K. Rohr. “On the Precision in Estimating the Location of Edges and Corners”, *Journal of Mathematical Image and Vision*, vol. 7, pp. 7–22, 1997.

[19] C. Schmid, R. Mohr and C. Bauckhage. “Comparing and Evaluating Interest Points”, In *Proceedings of the International Conference on Computer Vision*, pp. 230–235, Bombay, India 1998.

[20] A. Singh and M. Shneiner. “Gray Level Corner Detection: A Generalized and Robust Real Time Implementation”, In *Computer Vision, Graphics and Image Processing*, vol. 51, pp. 54–59, 1990.

[21] S. M. Smith and J. M. Brady. “SUSAN—A New Approach to Low Level Image Processing”, *International Journal of Computer Vision*, vol. 23, no. 1, pp. 45–78, May 1997.

[22] T. Stammberger, M. Michaelis, M. Reiser and K-H. Englmeier. “A hierarchical filter scheme for efficient corner detection”, *Pattern Recognition Letters*, vol 19, pp. 687–700, 1998.

[23] S. Tabbone. “Detecting Junctions Using Properties of the Laplacian of Gaussian Detector”, In *Proceedings of the 12th International Conference on Pattern Recognition*, vol. 1, pp. 52–56, Jerusalem, Israel 1994.

[24] M. Trajkovic and Mark Hedley. “Fast Corner Detection”, *Image and Vision Computing*, vol. 16, no. 2, pp. 75–87, Feb. 1998.

[25] D.M. Tsai, H.T. Hou and H.J. Su. “Boundary-based Corner Detection Using Eignevalues of Covariance Matrices”, *Pattern Recognition Letters*, 20(1):31-40, Jan. 1999.

[26] H. Wang and J.M. Brady. “Real-Time Corner Detection Algorithm for Motion Estimation”, *Image and Vision Computing*, vol. 13, no. 9, pp. 695–703, Nov. 1995.

[27] E.W. Weisstein. “CRC Concise Encyclopedia of Mathematics”, Chapman & Hall/CRC editor, 1999.

[28] O. A. Zuniga and R. Haralick. “Corner Detection Using the Facet Model”, In *Proceedings of IEEE Conference on Computer Vision and Pattern Recognition, Washington, DC (USA)*, pp. 30–37, June, Washington, USA, 1983.